ELSEVIER

Quaternary Science Reviews ▮ (▮▮▮▮) ▮▮▮–▮▮▮

QSR

Late Quaternary glaciation in the Kyrgyz Tien Shan

Michéle Koppes[a,*], Alan R. Gillespie[a], Raymond M. Burke[b], Stephen C. Thompson[c], John Stone[a]

[a]Department of Earth and Space Sciences, University of Washington, Seattle, WA 98195, USA
[b]Department of Geology, Humboldt State University, Arcata, CA 95521, USA
[c]William Lettis and Associates, Walnut Creek, CA 94596, USA

Received 16 May 2007; received in revised form 8 January 2008; accepted 11 January 2008

Abstract

The Tien Shan of Kyrgyzstan contains multiple moraines and drift from late Quaternary glaciations. The spatial/temporal distribution of the glaciers inferred from the moraines suggests that the main factor controlling glacier advance here was the availability of moisture. The dominant modern climatic signatures in northern Central Asia include orographic thunderstorms in summer, cold and dry Siberian high-pressure cells in winter, and westerly cyclonic storms from the North Atlantic and eastern Mediterranean in spring and fall. Changes in any of these systems during the late Quaternary would have varied precipitation delivery to, and glacier growth in the Kyrgyz Tien Shan. Geomorphic mapping and reconnaissance-level ^{10}Be cosmic-ray exposure dating of moraine sequences in six drainages indicate that there were multiple "maximum" advances of similar extents and equilibrium-line depressions across the range. Glaciers in the north and east of the Kyrgyz Tien Shan last advanced to their maximum positions during marine oxygen isotope stage (MIS) 5 and again during MIS 4, while in the south and west of the range advance occurred during MIS 3. In contrast to maritime Europe and North America, there is no evidence of a major glacial advance during MIS 2. Glacier advances during MIS 2 and since were restricted to the vicinity of modern glaciers, allowing the older glacial record to be preserved well.

1. Introduction

The most notable feature of the Quaternary Period has been its repeated climatic fluctuations, leading to advances and retreats of ice sheets, rise and fall of eustatic sea level, and many other geomorphic effects. Climate is in large part the sum of local and regional patterns of temperature and precipitation; thus, we might expect regional coherence in climate markers, but less coherence from region to region. Gillespie and Molnar (1995), for example, reported strong differences in the timing and extents of paleo-glaciers around the world. Because glaciers grow in response to local climatic conditions, it has been widely inferred that local conditions responsible for their growth can be garnered from their past extents, especially as these climatic conditions are converted to the equilibrium-line altitudes (ELAs), the altitude at which ice mass balance is zero. Glaciated valleys are numerous in the mountain belts of the world, and trend surfaces of the ELAs therefore can be well defined there. They can be used to infer paleo-climatic differences from one location to another, provided the glacial chronosequences have been dated. In particular, the regional variations in ELA can be used to determine temperature and precipitation gradients, allowing the reconstruction of current and former moisture sources and atmospheric circulation patterns (e.g., Burbank and Kang, 1991; Lehmkuhl, 1998).

Glaciers grow primarily in response to decreased summer temperatures and increased annual snowfall. Summer cloudiness can also be an important factor at high altitudes where sensible heat flux is inefficient and where sublimation may dominate (Rupper and Roe, 2007). Inferring past climate from ELA fluctuations is thus inherently ambiguous, requiring independent information to resolve. However, the sensitivity of glaciers to climate is

*Corresponding author. Department of Geography, University of British Columbia, Vancouver, BC, Canada V6W 1Z2.
Tel.: +1 604 822 3246 (off.).
E-mail address: koppes@geog.ubc.ca (M. Koppes).

0277-3791/$ - see front matter © 2008 Elsevier Ltd. All rights reserved.
doi:10.1016/j.quascirev.2008.01.009

not everywhere the same. In maritime areas, it is thought that glaciers grow primarily in response to increased snowfall. In more arid continental areas, glaciers are thought to grow primarily in response to cooling. Thus, the general climatic setting constrains the solutions to a degree. In addition, spatial variations in ELA depression at similar latitudes and altitudes can in principle be used to discriminate effects of temperature from those of precipitation, since the temperatures are not governed by storm tracks. In all settings, these factors vary in importance depending upon local geographic location and position downwind from local sources of moisture.

Central Asia, a mountainous region with a large distribution of alpine glaciers, has an extremely continental climate. Central Asia north of the Himalaya is beyond the reach of the Indian summer Monsoon. The dominant weather patterns are summer orographic thunderstorms, mid-latitude westerlies bringing cyclonic disturbances in the spring and fall, and winter thermal high-pressure systems that may act to divert storms along tracks south of the Himalaya (Fig. 1). The lofty Pamir and Karakorum ranges, each reaching 8 km in altitude, cause low-altitude air masses to diverge along northerly or southerly tracks around the high divide. During the Pleistocene, a more

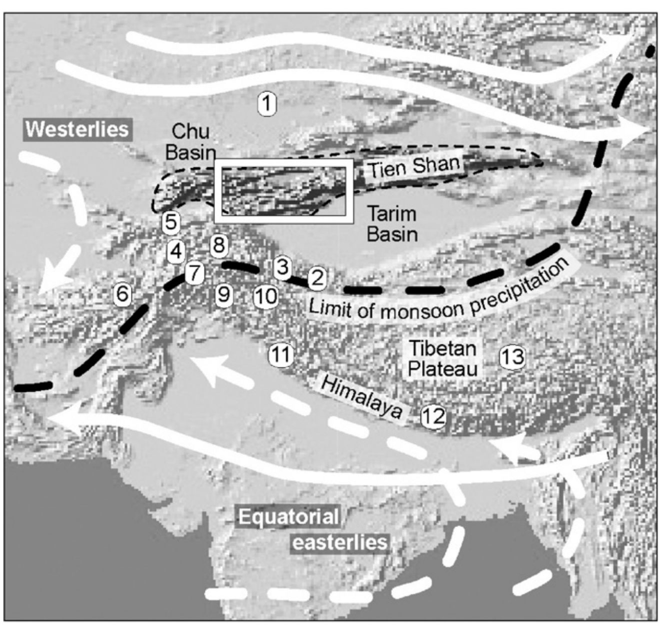

Fig. 1. Position of the Kyzgyz Tien Shan in Central Asia, areas of prior study of late Pleistocene glaciation referred to in text, and characteristic air circulation in the region. Solid white lines indicate air flow at around 3000 m, while dashed white lines indicate air flow around 600 m (after Benn and Owen, 1998). Dashed black line indicates modern extent of monsoonal precipitation in southern and Central Asia (after Shi, 2002). Locations of geographic features referred to in the text are shown by circled numbers: Lake Balkash (1), Kunlun mountains (2), Karakax valley (3), Pamir mountains (4), Alay Range (5), Hindu Kush mountains (6), Chitral district (7), Hunza Valley (8), Nanga Parbat peak (9), Karakorum mountains (10), Gahrwal Himalaya district (11), Mt. Everest (12), and Tanggula Shan mountains (13). Rectangle shows region of study in Kyrgyzstan (Fig. 2).

southerly jet stream increased selection of the southern track, presumably affecting the size of glaciers both north and south of the divide (e.g., Dodonov and Baiguzina, 1995; Hubberten et al., 2004).

The Tien Shan results from a distant convergence of the Indian and Asian tectonic plates (e.g., Thompson et al., 2002) and, like the Himalaya, comprises many separate smaller ranges. The Tien Shan forms the northernwestern edge of mountainous Central Asia, extending ~1500 km in a southwest–northeast arc from the western boundary of Kyrgyzstan (Kyrgyz Republic) through Xinjiang (China), almost as far east as Mongolia. The range trends approximately parallel to the major westerly storm tracks which pass from the North Atlantic and Mediterranean across the steppes of Kazakhstan and Uzbekistan, and acts as a topographic barrier to the storms (Hoskins and Hodges, 2002).

The prevailing winds in the Tien Shan are from the west and northwest (Liu and Han, 1992). The climate ranges from temperate in the northern foothills to semi-arid in the higher southern part of the range (Adyshev et al., 1987). Vegetation is sparse, consisting mostly of scrub steppe species; the high alpine basins, many of which lack significant vegetative cover, contain solely grasses. Precipitation in the northwestern Tien Shan occurs mainly in spring and fall; in the southeast, precipitation is mainly in summer (Aizen et al., 2001). Annual precipitation decreases north to south, from over 1000 mm/yr in the Kyrgyz Front Range (Kyrgyz Khrebet) to less than 300 mm/yr in the Aksai Basin (Fig. 2). The degree of storminess also decreases north to south: the Kyrgyz Front Range averages 110 days/yr with >1 mm of precipitation, while the southern basins average 70 days/yr. In contrast, the Terskey Ala Tau range, downwind from Issyk Kul, a large intermontane lake (Fig. 2), receives precipitation totaling 500 mm/yr that is spread over about half the year. Moisture evaporated from the lake may increase the number of rainy days, as well as modulate annual temperatures, there.

The Kyrgyz Tien Shan supports over 6000 modern glaciers on peaks ranging in altitude from 3000 to >7000 m a.s.l. It is well situated for the study of modern and paleo-glaciation in general, and to infer paleo-climatic conditions in a circumscribed setting that differs significantly from other ranges such as the Pamir (Abramowski et al., 2006) and Chitral (Owen et al., 2002b), which lie on the western edge of "High Asia" <500 km to the south. The position of the range, in a continental setting and outside the reach of the Indian Monsoon, permits meaningful testing of the "asynchronism" of global glaciations (Gillespie and Molnar, 1995), by providing a means of comparing the timing of local glacier advances in continental climates to those in more maritime settings. Deciphering the timing and magnitude of the late Pleistocene glaciations in the Kyrgyz Tien Shan will help us understand past climate conditions, in particular the influence of the mid-latitude westerlies and presence of the Siberian thermal

Please cite this article as: Koppes, M., et al., Late Quaternary glaciation in the Kyrgyz Tien Shan. Quaternary Science Reviews (2008), doi:10.1016/j.quascirev.2008.01.009

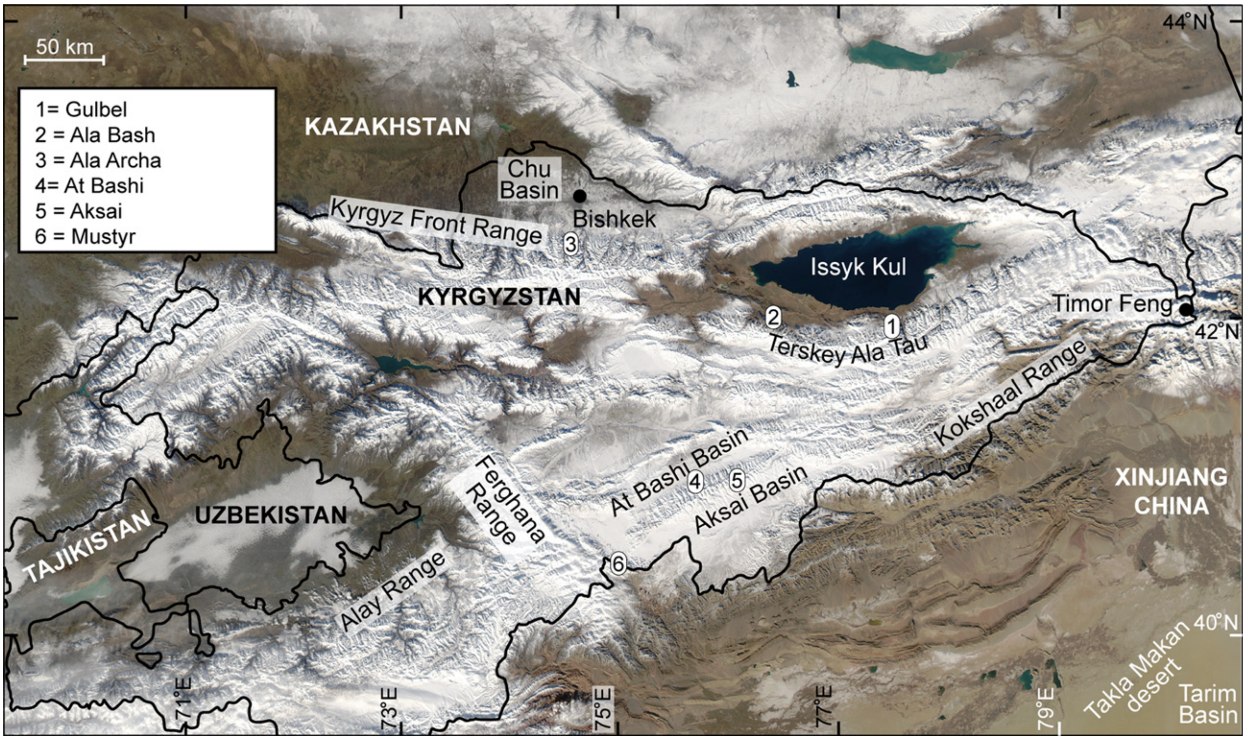

Fig. 2. MODIS image of Kyrgyzstan (rectangle in Fig. 1) showing the six areas of study and other geographic features named in the text. Circled numbers show the locations of the study areas: Gulbel (1), Ala Bash (2), Ala Archa (3), At Bashi (4), Aksai (5), Mustyr (6).

high-pressure system in delivering moisture to and modulating temperatures in the mountains of Central Asia.

2. Previous work

Until the early 1990s and the advent of numerical surface-dating techniques, it was generally assumed that alpine glacier advances in Central Asia were synchronous with those of the high-latitude ice sheets. As refined numerical dating techniques based on analysis of optical luminescence (OSL) and cosmogenic radionuclides (CRN) became widely applied, new studies are indicating that Asian glaciers advanced to their maximum extents at different times than the ice sheets in Europe or North America; there is even regional variability in the timing of glacial advances within Asia itself (e.g., Benn and Owen, 1998; Phillips et al., 2000; Finkel et al., 2003; Owen et al., 2005; Abramowski et al., 2006; Zhang et al., 2006).

A growing database of glacier chronologies for the Tibetan Plateau and adjacent mountain ranges presents a general picture of major glacier advances in the late Pleistocene becoming progressively less extensive with time. Comprehensive reviews (Finkel et al., 2003; Ehlers and Gibbard, 2004; Owen et al., 2005; Zhang et al., 2006) show that the local Last Glacial Maximum (LGM_L) for most of the Himalaya and Tibetan Plateau during the last 100-kyr glacial cycle pre-dates the "global" LGM (LGM_G) of MIS 2 (~25–12 ka) and probably occurred variously from MIS 5a–d (~130–75 ka) to MIS 3 (~60–25 ka). Abramowski et al. (2006) documented extensive advances in the Pamir and Alay ranges at 75–60 ka and 52–45 ka, but only smaller ones during the LGM_G. Sharma and Owen (1996) dated the LGM_L in northwestern Garwhal in the Central Himalaya at ~63 ka. Owen et al. (2005) and Schäfer et al. (2002) dated three extensive glacier advances in the Tanggula Shan of east-central Tibet to ~215, 105, and 68–46 ka. The end moraines of the last advance (LGM_L) were within 2–3 km of the present ice margins, suggesting only minor glacier advances during the "global" LGM_G. Lehmkuhl (1997) and Lehmkuhl and Haselein (2000) similarly found that LGM_G glaciers in central Tibet were not significantly larger than modern ones. Benn and Owen (1998) and Derbyshire et al. (1984) dated the last major glacial advance in the Hunza Valley to around 54–43 ka, with smaller advances around 26–22 ka and 18–15 ka. Similarly, using CRN and electron spin resonance (ESR), Yi et al. (1998, 2002), Zhao et al. (2002), and Zhou et al. (2002) dated the largest glacier advances in the Ürümqi River, Xinjiang Tien Shan, and the Qilian Shan at 73–50 ka, with progressively smaller advances around 42–35 ka and 25–15 ka. However, our own cosmic-ray exposure dating from the Ürümqi River and elsewhere in the Xinjiang Tien Shan (Gillespie et al., 1993a, b; Gillespie and Burke, 2000) indicates that MIS 2 and earlier advances were of about the same extent there.

Owen et al. (2005) attributed larger advances in the Hunza Valley, Khumbu Himal and NE Tibet during MIS 3 to a warm/wet regional climate and to a strong South Asian summer monsoon, which together with a summer insolation maximum would promote snowfall by both (1) increasing summer precipitation, and (2) raising winter temperatures. In contrast, subsequent smaller glacier advances during the LGM_G were attributed to reduced monsoon precipitation during the insolation minimum that acted to counter the potential increase in glacier mass balance due to a global drop in temperature (e.g., Lehmkuhl and Owen, 2005; Owen et al., 2005).

Little work on late Quaternary glaciation of the Kyrgyz Tien Shan has been conducted that includes chronologic data. Most of the studies there have focused on Holocene and Little Ice Age (LIA) glacier fluctuations (e.g., Bondarev et al., 1997; Savoskul, 1997; Solomina et al., 2004). Contemporary glaciers in the Kyrgyz Tien Shan indicate a pronounced gradient in response to a warming climate since the LIA, with a large retreat and rise in the ELA of the glaciers in the more humid northern and western part of the range, and minimal retreat in the arid south and east (Liu and Han, 1992; Savoskul, 1997; Solomina et al., 2004). The magnitude of the Holocene ELA depression in the Tien Shan, averaging 75–100 m during the LIA, is comparable to the ELA depression in more maritime settings (such as the Sierra Nevada) during the same period. The mass balance of the glaciers in the region is presumed to be driven mainly by summer temperature and spring and summer precipitation (Liu and Han, 1992), which are more pronounced in the north and south, respectively. The differences in impact of the amount of summer precipitation, in particular, is presumed to drive the variability in the gradient of ELA depression during the LIA (Savoskul, 1997) from 100 m in the northern part of the range to ~75 m in the south. Bondarev et al. (1997) also documented a precipitation increase around 11–10 ka ago and a later warming around 9 ka ago, recorded in the filling of lakes Balkash, Issyk Kul and Chatyr Kul. The early Holocene moisture and warming prompted a small glacier advance in the inner Kyrgyz Tien Shan, followed by a recession at ~8 ka, after which none of the glaciers re-advanced past their early Holocene maximum positions (Bondarev et al., 1997).

3. Study areas

We selected six glaciated drainages in the Kyrgyz Tien Shan for study and dating. The six sites represent a variety of climatic zones along north–south and east–west transects through the range (Fig. 2). Each site contains chronosequences of glacial drift that record the maximum glacier extents of the late Quaternary. Due to limited funding, we were unable to date all the CRN samples we collected, and therefore our dating is at the reconnaissance level.

Climatic and environmental data for study areas are summarized from Adyshev et al. (1987). Altitudes are from topographic maps and NASA's 90-m Shuttle Radar Topographic Mission digital elevation models (DEM) (Farr and Kobrick, 2003).

3.1. Gulbel—42°02′N, 76°09′E

The Gulbel study area anchors the eastern end of the E–W study transect. It lies astride the low 3300-m Gulbel Pass south of Issyk Kul. The pass divides east- and west-trending valleys that parallel the crest of the Terskey Ala Tau, a ridge of high peaks to the south averaging >4000 m in altitude. The basin elevation of the Korumdy Valley is ~2350 m. Mean annual precipitation (MAP) averages 500 mm, falling mainly in spring and summer. Air temperatures near the pass, based on published values for the center of the basin and corrected for adiabatic cooling, range annually from −14 to 12 °C. Bedrock is granitic, and vegetation cover is grass.

The Korumdy River flows north from the crest to the vicinity of Gulbel Pass, where it turns west. The Terskey Ala Tau was heavily glaciated in the Pleistocene, and modern glaciers spill out of their cirques. The ridge north of Gulbel Pass, however, is lower (~3500 m) and was not glaciated, although northeast-facing valleys show signs of permafrost and solifluction above 3000 m. Pleistocene glaciers advancing out of the Terskey Ala Tau along the Korumdy drainage overtopped Gulbel Pass, and flowed east. They later changed direction and flowed west, down the valley of the Korumdy River to around 2530 m.

3.2. Ala Bash—42°05′N, 76°27′E

The Ala Bash study area is 60 km west of Gulbel Pass in the same tectonic and geographic setting. Peak heights average 4110 m. The Ala Bash Basin also is lower (2090 m) than the Korumdy Valley. MAP is ~400 mm, falling mainly in spring and summer. The ridges are snow-covered from October to April. Annual temperatures in the basin are modulated by the proximity to lake Issyk Kul and range from −9 to 17 °C, with minima as low as −20 °C. Bedrock is granitic, and vegetation cover is grass.

Modern glaciers near Ala Bash are restricted to their cirques. Within 2 km downstream are fresh-appearing moraines, and moraines of older valley glaciers extend to the edge of the Ala Bash Basin, at 2170 m. Several generations of moraines are present.

3.3. Ala Archa—42°32′N, 74°31′E

The Ala Archa drainage is on the north side of the Kyrgyz Front Range, just south of the capital city, Bishkek. Ala Archa anchors the northwest end of our transect, and of all the sites we visited is the most directly exposed to moisture-bearing storms. Near Ala Archa, the Kyrgyz Front Range is >4000 m in altitude; the Chu Basin at the foot of the range, where Bishkek lies, is at 1200 m. MAP is >1000 mm/yr, a factor of 2 greater than in the Terskey Ala Tau. Precipitation falls mainly in spring and fall. Typical monthly temperatures range from −4 to 24 °C, with maximum summer temperatures as high as 44 °C. Bedrock is dominantly schist.

Please cite this article as: Koppes, M., et al., Late Quaternary glaciation in the Kyrgyz Tien Shan. Quaternary Science Reviews (2008), doi:10.1016/j.quascirev.2008.01.009

The northern slopes of the Kyrgyz Front Range are deeply incised, and the highest peaks lie in a zone up to 11 km north of the watershed divide. The slopes and valleys are forested, with grasslands at the lower altitudes.

Glaciers in the Kyrgyz Front Range overflow their cirques, and the U-shaped profiles of the incised valleys suggest extensive Pleistocene glaciation. Young moraines are preserved within 2 km of the modern glacier termini. Although some older moraine fragments have been preserved, most Pleistocene drift appears to have been eroded from the steep slopes.

3.4. At Bashi—41°03′N, 75°45′E

The At Bashi Range comprises the east–west spine of the southern Kyrgyz Tien Shan, separating the At Bashi (north) and Aksai (south) basins. Our study area is the Terekçu Valley, on the northern flank of the range. Peak altitudes in the Terekçu headwaters are as high as 4600 m; the altitude of the basin at the range front is 2150 m. MAP is ~400 mm/yr, with precipitation falling mainly in spring and summer. Monthly temperatures range from −15 to 17 °C. Bedrock is granite and schist. Vegetation is grass and low shrubs.

Well-preserved sequences of moraines are seen in most of the drainages of the At Bashi Range, and end moraines occur on the piedmont. Older moraines protrude from beneath the largest LGM_L moraines. Modern cirque glaciers are common. There appear to be no moraines between the moraines near the range front and the cirques.

3.5. Aksai—41°01′N, 76°03′E

The Aksai Basin is the southernmost basin of the Kyrgyz Tien Shan, adjacent to the Tarim Basin and the Taklamakan desert in Xinjiang. The study area is southeast of the Terekçu Valley, in the south-flowing Djo Bog Gulsh drainage. Crest altitudes are ~4200 m; basin altitude averages 3240 m. MAP is ~275 mm/yr, with precipitation falling mainly in summer. Monthly temperatures in the basin typically range from −26 to 8 °C and average −10 °C at the modern ELA (~4150 m), but winter temperatures can be as low as −54 °C. Bedrock is granite and schist, and vegetation is grass.

Access to the southern basin is limited because of proximity to the border with China. The relatively accessible northern piedmont has an extensive set of faulted and folded terraces below large moraines that extend beyond the range front (Thompson et al., 2002). Solifluction features are abundant on the mountain slopes, but not on the moraines. There are no clean-ice glaciers in the drainage, although there are a few rock glaciers. Glaciers do occur to the west, where the range is higher.

3.6. Mustyr—40°36′N, 75°03′E

The Mustyr drainage is the southern end of our N–S study transect. The study site is west of Torgurat Pass, a major trade route to China before political considerations effectively closed the border. It is located where the Mustyr River leaves the Torgurat Range, which rises to >4800 m. The Torgurat Range is the southernmost high ridge of the Kyrgyz Tien Shan and borders the southern end of Aksai Basin. The northern slopes are deeply incised and glaciated; the southern slopes are steeper and largely unglaciated. The Torgurat Range continues northwestward as the Ferghana Range, which defines the western edge of the basin-range topography of the Kyrgyz Tien Shan. Basin altitude is ca 3350 m. Vegetation is grass, and MAP is ~300 mm/yr, with precipitation falling mainly in summer. Bedrock is marble and schist, with very little quartz available for ^{10}Be analysis, and hence although sampled no boulders have been dated from this location at this time.

Large Pleistocene moraines and broad fluvial/outwash terraces occupy the piedmont below the mountain front, and ice-contact drift is seen between the Mustyr River and Chatyr Kul, a large shallow lake. Glaciers occupy the cirques and upper valleys of the Torgurat Range, but these lie close to the political border with China and during the time of the field campaign could not be investigated.

4. Approach

Drift and glacial landforms at each study site were mapped in the field and from satellite images and Russian air photos to interpret the local glacial history. Boulders from moraine crests were sampled for cosmic-ray exposure dating, and elevations of key features were measured using GPS and SRTM DEMs to calculate paleo- and modern ELAs. Field mapping was done in August–September 1998 and 2001. In 1998, mapping was on a satellite image base (Corona) and 1:200,000-scale Russian topographic maps, where available. After the 1999 launch of NASA's Terra satellite, 15-m ASTER images became available and were used to refine the geological maps.

Moraines of five ages were mapped according to relative age assignments designated by allostratigraphic position, morphology, relative dating of moraine and terrace surfaces, and cosmic-ray exposure dating. Criteria are summarized in Table 1. The LGM_L moraines are defined as dating from the last glacial cycle (<MIS 6) and in some valleys are simply the moraines farthest from the headwall, which commonly extended in a piedmont lobe from the valleys into the basins. However, in some of the valleys eroded and subdued MIS 6 or older moraines were found farthest downvalley, often discontinuous and protruding at an angle from beneath the most prominent piedmont. In such cases the LGM_L moraine was taken to be the most pronounced, well-defined lateral and/or terminal moraine that overlay any of the more subdued moraines. This

Table 1
Field criteria for designation of glacier advances I–V, based on stratigraphic and morphologic relations

Relative age of moraines	Morphological criteria for designation
I	Oldest moraine sequence in valley. Commonly on piedmont, extends from beneath largest, most well-defined lateral moraine, but terminates at similar altitude. A, B, and C soil horizons are well defined; significant carbonate deposition in C horizon. Loess cap is >2 m and extensive. Few tillstones are exposed: granitic tillstones are eroded and near the soil surface; schist tillstones are shattered.
II	Penultimate local maximum glacial advance. Commonly in piedmont form, extends from beneath largest, most well-defined lateral moraine. A, B, and C soil horizons are well-defined, significant carbonate deposition in C horizon. Loess cap is >2 m and extensive. Boulders at surface are partially buried, some evidence of spallation. Often contain kettle topography and other evidence of ice stagnation.
III (III_a, III_b)	Local Last Glacial Maximum (LGM_L) advance. Moraines are large and well defined, and the lateral moraines extend out from the upper valleys and into the basins. Moraine crest is rounded, till-mantled with large boulders protruding, and capped with 1–2 m of loess. The lateral moraines encompass stagnant ice features and are often inset with smaller recessional moraines. III_a and III_b are similar appearing but where mapped III_a is overlain by III_b.
IV	Largest cirque/upper valley glacial advance. Moraines are found within a few kilometers of extant glaciers, and do not extend past the range front. Moraines are smaller, till is mostly clast-supported, and sparsely vegetated. Soils contain incipient A and B soil horizons. Moraine crests are sharp and boulder-strewn, with slopes of between 20° and 30°.
V	Highest paleo-moraine, adjacent to modern glacier, often enclosing modern glacier terminus within 1–2 km. Moraine crest is sharp, till is clast-supported. Slopes of moraine exceed 30°. No less and no soil development on moraine are evident.

moraine was commonly characterized by the presence of significant numbers of large boulders along a parabolic crest. We also recorded the thickness and character of the till and of the loess by hand-excavating 1.5–2-m pits on moraine crests and characterized the soil profile and imbedded tillstones. Depths and soil horizons in loess caps were measured and recorded.

We estimated modern and paleo-ELAs for our study areas. Given the geological complexities of the study region, especially the presence of tributary glaciers and outlet glaciers, together with the lack of high-resolution topographic data, we adopted the simple Toe-Headwall Altitude Ratio (THAR) method (Meierding, 1982) for estimating the ELAs. Modern terminus and headwall altitudes were calculated from 80-m contours on the topographic maps and verified from late summer snowlines visible on the Corona images. Terminus altitudes for former glaciers were taken from GPS measurements on the crest of LGM_L end moraines. Ratios of 0.40 (northern and eastern Tien Shan) and 0.55 (central and southern Tien Shan) were used for modern glaciers, as recommended by Savoskul (1997). Errors of ± 80 m are estimated from the discordance from method to method, accuracies and precisions for the maps, and published estimates (e.g., Gillespie, 1991; Benn et al., 2005).

The highest altitude of LGM_L lateral moraines also provides an estimate of the paleo-ELA. It was measured where possible and compared to the THAR-derived ELA, which appeared to be lower by up to 400 m in the northern and eastern Tien Shan, and higher by up to 150 m in the south. This difference may indicate a change in the relative significance and spatial variance of avalanching, sublimation and melting in controlling glacier mass balance between the late Pleistocene and today. Contributions of debris cover and avalanching can significantly influence the mass balance of alpine glaciers (Benn and Lehmkuhl, 2000; Owen and Benn, 2005), and must be considered in estimating paleo-ELAs accurately, by any method. Because we were unable to infer these contributions for prior glacial advances, and not enough information on the elevation of the highest lateral moraines was available to accurately adjust paleo-THAR ratios across the region, our THAR-derived ELA values should be regarded as lower limits.

Rock samples of ~0.5 kg for cosmic-ray exposure dating were chiseled from the tops of boulders on moraine crests. To reduce the possibility of burial/exhumation histories and shielding by snow, boulders sampled were >1 m high above the moraine surface. Locations were chosen where there was no apparent burial, fire spallation, erosion, or solifluction. In practice, ideal samples were rarely available and compromises were necessary, especially in boulder size. Not all drainages had quartzose clasts for ^{10}Be analysis, in which case marble or schist samples were collected for future ^{36}Cl analysis. GPS and map locations were measured and recorded as each site, sample sites were photographed, and the horizon, topographic slopes, erosion features, vegetation cover, shape/size of sampled boulders, erosion relief, and pits were all measured and recorded. Given the geographic breadth of the study area, and funding constraints, a pragmatic decision was made to date as many moraines as possible, rather than investing the available dates on a single chronosequence.

Samples were prepared at the University of Washington and then measured for ^{10}Be at the Center for Accelerator Mass Spectroscopy at Lawrence Livermore National Laboratory. Preparation methods followed Stone (2004) and Nishizumi et al. (1989). Measured isotope ratios were converted to ^{10}Be concentrations in quartz using the total ^{10}Be in the sample and the sample weights, following Stone (2004). The concentrations were then converted to cosmic-ray exposure ages using the CRONUS-EARTH Version 1.2 surface exposure-age calculator (url: http://hess.ess.washington.edu/math), which uses the sea-level high-latitude production rate of 5.15 atom/g_{qtz}/yr (Stone, 2000). Production rates were scaled to the latitude and altitude of the

Please cite this article as: Koppes, M., et al., Late Quaternary glaciation in the Kyrgyz Tien Shan. Quaternary Science Reviews (2008), doi:10.1016/j.quascirev.2008.01.009

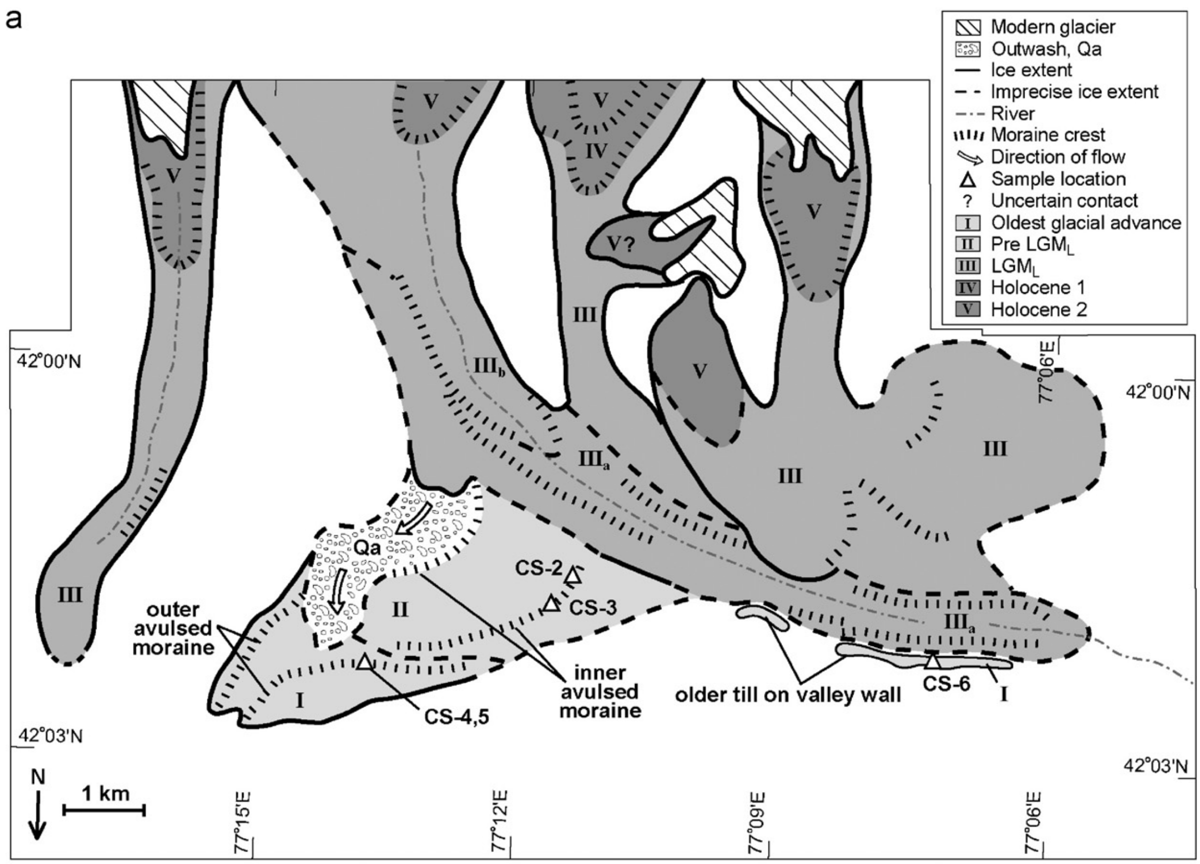

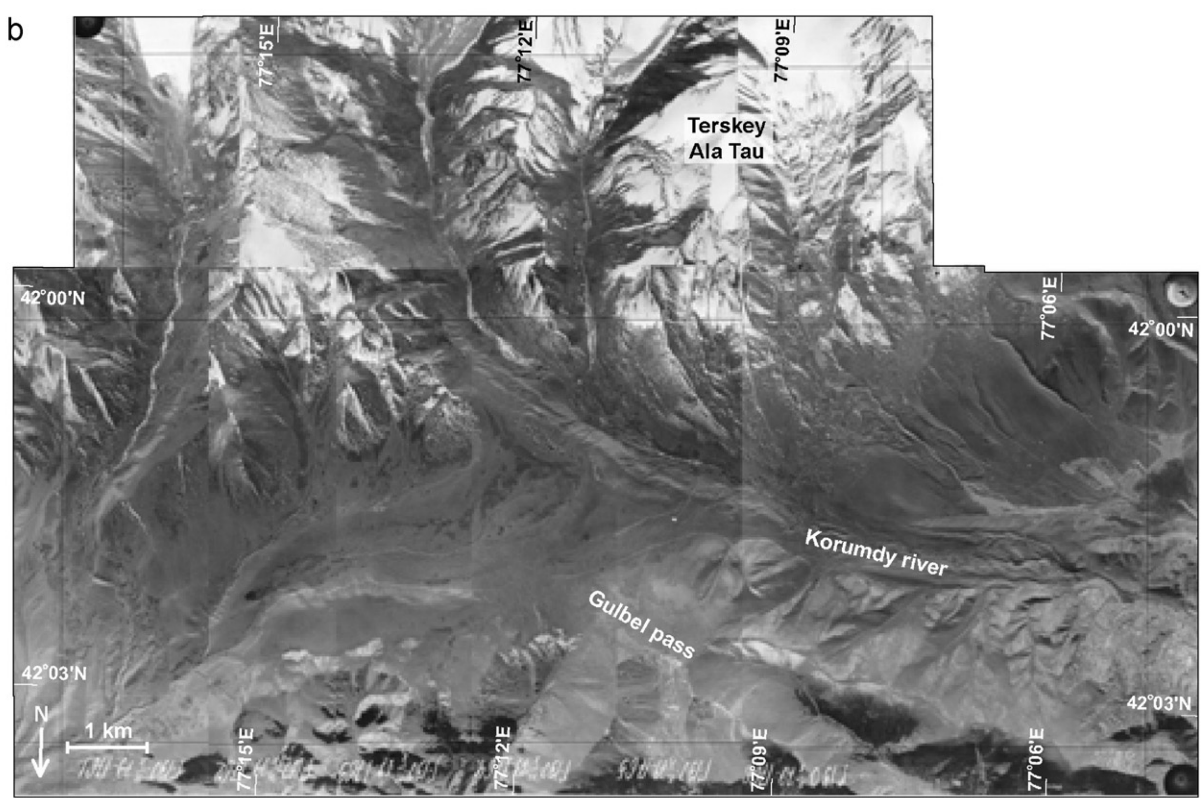

Fig. 3. The Gulbel study area on the Korumdy River. (a) Map of glacier extents and related landforms and deposits, including CRN sample localities. "Modern glaciers" include rock glaciers. (b) Aerial photographs (Γ-130-11/x79-1761 through 1766). (c) Legend for maps in Figs. 3–6. Criteria for designating Units I–V is discussed in Table 1.

sampling sites, following Lal (1991), and a correction factor was applied for sample thickness, shielding, and erosion. "Minimum" and "maximum" exposure ages were calculated for each site, assuming a minimum erosion and burial history ("min": erosion rate 1 mm/ka, no burial) and a maximum erosion and/or burial history ("max": erosion rate 3 mm/ka, or burial for significant periods), as have been used by others in the region (e.g., Clark et al., 2001; Finkel et al., 2003; Abramowski et al., 2006).

5. Results

Geologic maps and satellite images of the study areas are given in Figs. 3–6. Cosmic-ray exposure dates are presented in Table 2; modern and paleo-ELAs are presented in Table 3 and Fig. 7.

5.1. Gulbel (Fig. 3)

Field study was restricted to the vicinity of the road crossing Gulbel Pass (3350 m); mapping within the Terskey Ala Tau largely involved photo-interpretation. The late Pleistocene moraines (Units I–III) on Gulbel Pass are smooth and rounded, and capped by up to 1 m of loess. The lowest end moraines are at an altitude of 2620 m. Drift on the valley floor is minimal, and there is no stagnant-ice terrain. Moraines of two units, I and II, were deposited east of Gulbel Pass, ending at altitudes of 3050 and 3220 m, respectively. It is not clear if the glacier that formed the moraines flowed only east across the pass, or bifurcated. Old drift (of Unit I?) is also found on the south wall of the Korumdy Valley above a pronounced Unit III right-lateral moraine. The Unit III (LGM_L) moraines are found only in the Korumdy Valley where the ice flowed NW; the glacier responsible for their deposition did not overtop the pass, but instead downcut across the Unit I and II moraines.

Upvalley from Gulbel Pass, end moraines from a younger glacier are found at 3240 m. We assigned this moraine to a Unit IV advance, but it is possibly a LGM_L recessional moraine. Closed moraines of Unit V are found at 3590 m, ~2 km from the modern glaciers (termini at ~3700 m). The active glaciers have clean ice.

Boulders on moraines I and II were few in number and did not generally meet the criteria for cosmic-ray exposure dating, being low to the surface and weathered. Two boulders from each of the moraines I and II were dated. Apparent ages were discrepant, but the older from each moraine was similar: 72 ka (Unit I) and 77 ka (Unit II). A single suitable boulder was found on the Unit I drift in the Korumdy Valley and appears to be much older: 155 ka. No boulders were discovered on the LGM_L (Unit III) moraine itself. Because of erosion and the potential for burial and exhumation, the "max" values are taken as an approximate lower limit for the moraine ages.

The ELA for the modern glaciers of the Korumdy River drainage is ~3960 m. The ELA for the LGM_L (III) west-flowing glacier was ~3180 m, a depression of 780 m relative to the modern ELA. The ELAs for the east-flowing glaciers I and II were 3610 and ~3690 m, for depressions of 350 and 270 m, respectively; thus, they were less extensive than the Korumdy LGM_L.

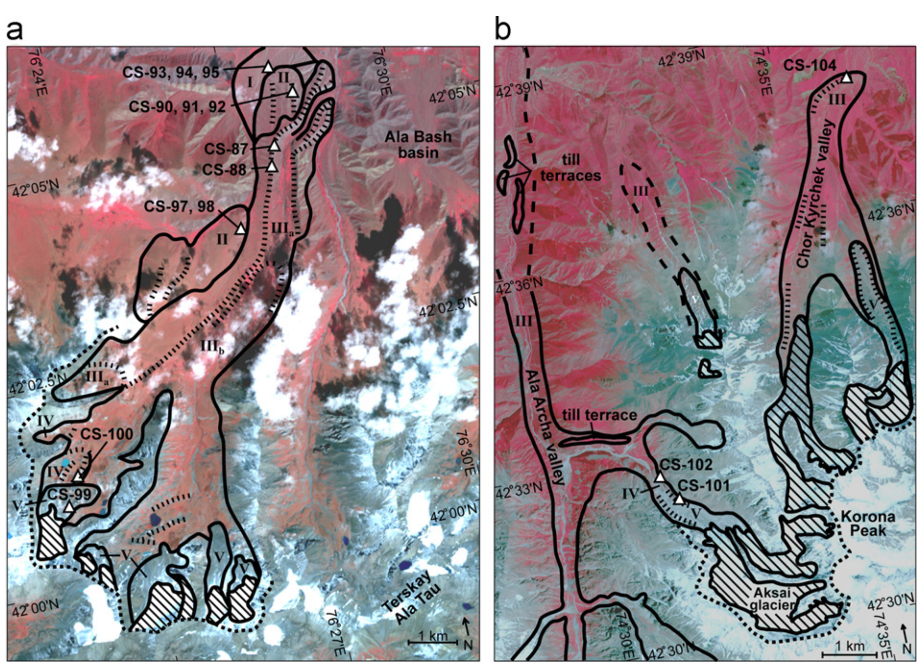

Fig. 4. The Ala Bash and Ala Archa study areas: maps of glacier extents and related landforms and deposits, including CRN sample localities, overlain on Terra ASTER images. Dotted lines indicate drainage divides. (a) The Ala Bash Basin, Terskey Ala Tau Range: image AST_L1B.003:2004082451. (b) The Ala Archa and Chor Kyrchak Valleys, Kyrgyz Front Range: image AST_L1B.003:2017930226.

Please cite this article as: Koppes, M., et al., Late Quaternary glaciation in the Kyrgyz Tien Shan. Quaternary Science Reviews (2008), doi:10.1016/j.quascirev.2008.01.009

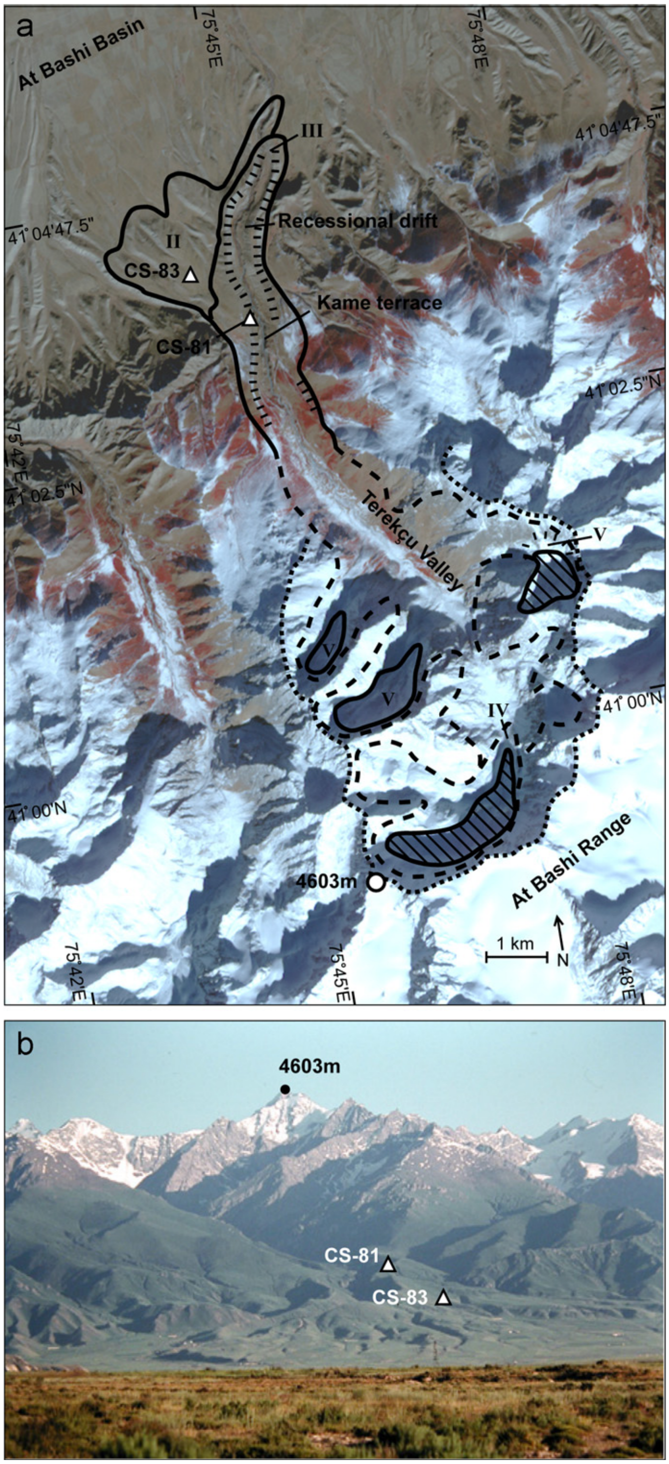

Fig. 5. The At Bashi study area overlain on Terra ASTER: image AST_L1B.003:2010410788. (a) Map of glacier extents and related landforms and deposits, including CRN sample localities. (b) Photograph of piedmont moraine sequence and the At Bashi Range, taken looking south across At Bashi Basin.

5.2. Ala Bash—(Fig. 4a)

The moraines of the Ala Bash Basin extend down to the piedmont, at an altitude of ~2200 m. Although they appear smooth and rounded, and are mantled by up to 50 cm of loess, many boulders occur on the crests. The terminus area is complex, with older I and II end moraines extending a short distance from beneath the III_a (LGM_L) left-lateral moraine near its end. Permafrost was not encountered in the soil pits on the moraines and there are no slumps, sediment lobes, or other solifluction features: i.e., cryoturbation appears to have been negligible. The degree of soil development was much greater on the older moraines than for the LGM_L moraine. Below an inset recessional III_b moraine at ~2830 m, the moraines form simple ridges, with little ground moraine in the glacial trough. Above III_b, however, is a terrace with kettles, eskers, complex ridges, and outwash, and it appears that the debris load increased at the end of the LGM_L.

Another remnant of a Unit II left-lateral moraine extends from beneath the III_a left-lateral and terminates at 2690 m, ~400 m higher than the Unit I and II end moraines. Given the difference in elevation, it is improbable that both Unit II moraines were left by the same advance. The few exposed boulders on both Units II were low (< 1 m) to the surface and appeared deeply weathered; therefore, exposure ages probably underestimate the moraine age.

Above the recessional moraine (III_b) is a basin fed by six cirques. The westernmost cirque contains a lightly weathered till terrace and an arcuate moraine (Unit IV) below an ice-cored moraine (Unit V); an active rock glacier lies ~250 m above this Unit IV moraine. There was no loess found in the cirque.

Three exposure ages ("max") from moraine I ranged widely, from 197 to 83 ka. Similarly, end moraine (Unit II) yielded four apparent ages of 260–81 ka, and left-lateral moraine (Unit II) at 2690 m gave ages of 113 and 55 ka. None can be trusted as landform ages; however, all must predate Unit III_a, for which the ages of 80 and 73 ka may be closer limits to the age of the last major advance. No suitable CRN samples were found on recessional moraine III_b. A single suitable sample at moraine IV (CS-99) in the upper cirque was dated at 18 ka ("min"), and a single sample from moraine V provided a date of 3 ka. Although these single dates are not definitive, we suspect they are landform ages because the sampled rocks were unweathered, with no indication of burial or exhumation. If correct, the moraine of Unit IV dates from the LGM_G.

The ELA for the LGM_L and pre-LGM_L glaciations was ~2900 m, 200 m lower than at Gulbel. The LGM_L ELA depression was 1100 m relative to the modern glaciers. The ELA for the Unit IV (MIS 2) moraine was 3850 m, a depression of only 150 m.

5.3. Ala Archa (Fig. 4b)

The Ala Archa Valley was extensively glaciated down to an altitude of ⩽1580 m during the Pleistocene. The glaciers were confined to the steep canyons of the Kyrgyz Front Range. Remnant benches, possibly underlain by till or outwash, extend to an altitude of 1400 m near the mouth of

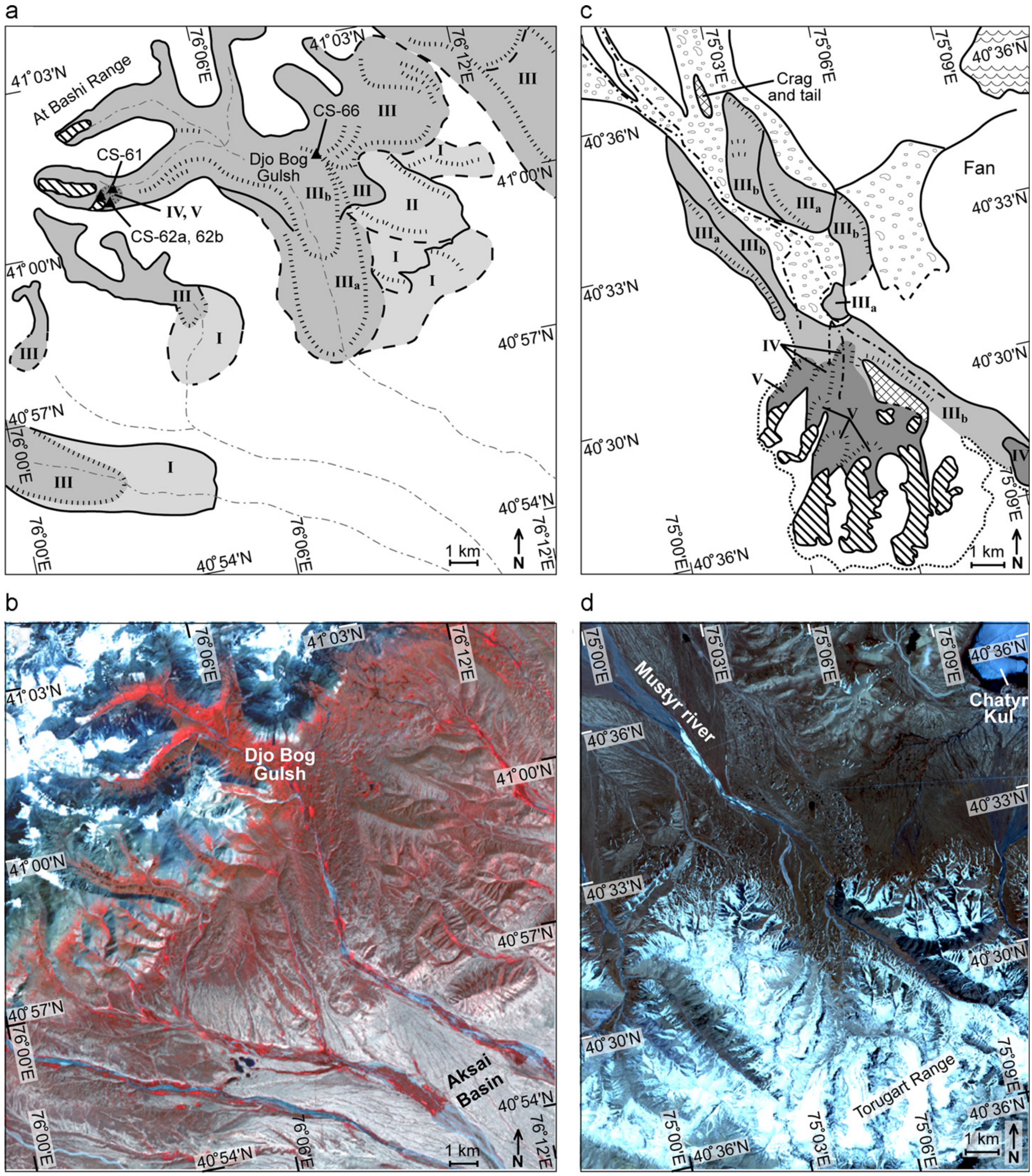

Fig. 6. The Aksai and Mustyr study areas: maps of glacier extents and related landforms and deposits, including CRN sample localities, and Terra ASTER images. (a) Aksai map. (b) Aksai: image AST_L1B.003:2004069916. (c) Mustyr map. (d) Mustyr: image AST_L1B.003:2003136436.

the canyon, but they are heavily eroded and forested, and could not be sampled. The only well-preserved moraines are in cirques, within a few kilometers of the modern glaciers, and appear similar in size and morphology to the cirque moraines of Ala Bash (IV and V). Only these moraines were sampled for cosmic-ray exposure dating.

Please cite this article as: Koppes, M., et al., Late Quaternary glaciation in the Kyrgyz Tien Shan. Quaternary Science Reviews (2008), doi:10.1016/j.quascirev.2008.01.009

Table 2
^{10}Be cosmic-ray exposure ages from the Kyrgyz Tien Shan

Sample ID	Location	Latitude (°N)	Longitude (°E)	Altitude (m)	Geographic scaling factor	Rock type	Sample thickness (cm)	Topographic shielding factor	^{10}Be concentration[a] ($\times 10^5$ atoms/g_{qtz})	^{10}Be exposure age[b,c] (min) (ka)	^{10}Be exposure age[d] (max) (ka)
SCT/020901/2	Gulbel	42.03	77.19	3283	10.5928	Granite	1	0.9916	20.11±0.49	40.5±3.1 (1.0)	76.8±6.9 (2.3)
SCT/020901/3	Gulbel	42.03	77.19	3283	10.5928	Granite	1	0.9916	16.23±0.41	32.4±2.4 (0.8)	59.2±5.1 (1.8)
SCT/020901/4	Gulbel	42.04	77.21	3140	9.7466	Granite	1	0.9916	13.88±0.35	30.0±2.3 (0.7)	49.3±4.1 (1.4)
SCT/020901/5	Gulbel	42.04	77.21	3140	9.7466	Granite	1	0.9916	19.10±0.57	41.9±3.3 (1.3)	72±6.6 (2.6)
SCT/030901/6	Gulbel	42.04	77.12	2759	7.7342	Granite	1	0.9916	33.48±0.80	98.1±7.9 (2.6)	155.1±17.7 (5.9)
KTS98-CS-61b	Aksai	41.00	76.05	3804	13.8482	Granite	3	0.9897	5.07±0.15	7.6±0.6 (0.2)	7.4±0.6 (0.2)
KTS98-CS-62a	Aksai	41.00	76.05	3879	14.4118	Granite	3	0.9897	3.20±0.10	4.6±0.3 (0.1)	4.7±0.4 (0.1)
KTS98-CS-62b	Aksai	41.00	76.05	3879	14.4118	Granite	3	0.9893	3.05±0.09	4.4±0.3 (0.1)	4.5±0.3 (0.1)
KTS98-CS-66	Aksai	40.98	76.15	3576	12.2293	Qtz vein in schist	4	0.9964	20.58±0.35	36.5±2.7 (0.6)	39±3.1 (0.7)
KTS98-CS-81	At Bashi	41.05	75.73	2598	6.8561	Qtz vein in schist	1	0.9980	10.32±0.25	31.6±2.4 (0.8)	33.5±2.7 (0.9)
KTS98-CS-83	At Bashi	41.05	75.73	2598	6.8561	Qtz vein in schist	1	0.9981	16.77±0.42	52.5±4.0 (1.4)	58±5 (1.7)
KTS98-CS-87	Ala Bash	42.08	76.46	2496	6.5479	Granite	0.5	0.9974	19.35±0.23	64.0±4.8 (0.8)	72.5±6.2 (1.1)
KTS98-CS-88	Ala Bash	42.08	76.46	2496	6.5479	Granite	4	0.9974	20.40±0.34	69.9±5.3 (1.3)	80.3±7.1 (1.7)
KTS98-CS-90	Ala Bash	42.08	76.46	2403	6.1623	Granite	7	0.9981	33.77±1.49	134.6±12.7 (6.9)	187.9±26.8 (14.5)
KTS98-CS-91	Ala Bash	42.08	76.46	2403	6.1623	Granite	2	0.9999	41.60±0.97	163.5±14.1 (4.6)	259.6±41.7 (13.5)
KTS98-CS-92	Ala Bash	42.08	76.46	2403	6.1623	Granite	5	0.9938	19.05±0.46	70.2±5.5 (1.8)	80.7±7.4 (2.4)
KTS98-CS-93	Ala Bash	42.08	76.45	2229	5.4889	Granite	5	0.9935	22.95±0.62	97.7±8.0 (2.9)	120.8±12.6 (4.6)
KTS98-CS-94	Ala Bash	42.08	76.45	2229	5.4889	Granite	2.5	1.0000	25.88±0.73	108.4±9.0 (3.4)	138.3±15.3 (5.8)
KTS98-CS-95	Ala Bash	42.08	76.45	2229	5.4889	Granite	3.5	1.0000	31.90±0.62	139.0±11.5 (3.2)	197.4±25.4 (7)
KTS98-CS-96	Ala Bash	42.08	76.45	2229	5.4889	Quartzite	10	0.9999	16.81±0.40	72.2±5.7 (1.9)	83.4±7.7 (2.6)
KTS98-CS-97	Ala Bash	42.05	76.43	2850	8.1846	Granite	1	0.9981	34.00±0.79	93.0±7.4 (2.4)	113.4±11.4 (3.7)
KTS98-CS-98	Ala Bash	42.05	76.43	2850	8.1846	Granite	2	0.9980	18.99±0.45	50.1±3.8 (1.2)	55.1±4.6 (1.5)
KTS98-CS-99	Ala Bash	42.05	76.43	3750	13.7581	Granite	2	0.9959	2.26±0.07	3.4±0.3 (0.1)	3.4±0.3 (0.1)
KTS98-CS-100	Ala Bash	42.05	76.43	3750	13.7581	Granite	6	0.9959	11.32±0.27	17.8±1.3 (0.4)	18.3±1.4 (0.5)
KTS98-CS-101	Ala Archa	42.52	74.51	3246	10.0749	Granite	2	0.9288	0.12±0.03	0.25±0.1 (0.1)	0.24±0.1 (0.1)
KTS98-CS-102	Ala Archa	42.52	74.51	3180	10.4714	Granite	1.5	0.9125	0.25±0.04	0.54±0.1 (0.1)	0.54±0.1 (0.1)
KTS98-CS-104	Chor Kyrchak	42.63	74.61	2040	4.8709	Quartzite	3	0.9966	10.90±0.39	48.7±4.0 (1.9)	53.4±4.8 (2.2)

[a]Measured ^{10}Be nuclide concentration relative to LLNL in-house ^{10}Be/^{9}Be standards, traceable to ICN ^{10}Be standard. Uncertainties were propagated at $\pm 1\sigma$ level including all known sources of analytical error.

[b]Simple exposure ages, assuming no prior exposure during ^{10}Be accumulation, calculated using CRONUS EARTH version 1.2 (Balco and Stone, 2006; Balco et al., 2007). Uncertainties are $\pm 1\sigma$ (68% confidence) including ^{10}Be measurement uncertainties and an assumed uncertainty of $\pm 6\%$ in the ^{10}Be production rate, to allow comparison with ages obtained using other methods. Values in parentheses are uncertainties based on measurement errors alone. Topographic shielding and paleo-magnetic corrections were calculated from CRONUS EARTH v.1.2. Sample density used is 2.7 g/cm^3.

[c]Minimum exposure age based on erosion rate of 0.0001 cm/yr.

[d]Maximum exposure age based on erosion rate of 0.0003 cm/yr, and/or burial and subsequent exposure due to moraine degradation or loess deposition.

Table 3
Snowline and ELA elevations (m) of modern and paleo-glaciers for the major mountain ranges studied

Range	Unit III$_a$ (LGM$_L$)			Unit III$_b$ (LGM$_L$)			Unit IV (Holocene)	
	Terminus altitude	ELA (THAR$_{0.4}$)[a]	Highest moraine[b]	Terminus altitude	ELA (THAR$_{0.4}$)[a]	Highest moraine[b]	Terminus altuitude	ELA (THAR$_{0.4}$)[a]
(a) Paleo-glaciers								
Terskey Ala Tau								
Gulbel	2620	3180	3530	2620	3180	3530		
Ala Bash	2200	2950	3350	2200	2950	3350		3850
Kyrgyz Front Range								
Ala Archa								3350
Chor	2040	2450		2040	2450			
Kyrchak								
At Bashi Range								
At Bashi	2415	2960	3115	2415	2960	3115		
Aksai	3380	3750	3580	3380	3750	3580		
Torugart Range								
Mustyr	3450	3931	3890	3450	3931	3890		

Range	Aspect	Glacier toe altitude	Headwall altitude	Snowline altitude[d]	ELA (THAR$_{0.4}$)[a]	ELA (THAR$_{0.55}$)[c]
(b) Modern glaciers and rock glaciers						
Terskey Ala Tau	N	3560	4250		3836	3940
	N	3560	4250		3836	3940
	SW	3620	4250		3872	3967
	NNW	3500	4500		3900	4050
	NW	3300	4600		3820	4015
	SSW	3600	4480		3952	4084
	S	3520	4560		3936	4092
	SW	3800	4350		4020	4103
	N	3620	4480		3964	4093
	NE	3800	4400		4040	4130
	N	3480	4520		3896	4052
	SE	3400	4400		3800	3950
	N	3600	4350		3900	4013
	N	3400	4200		3720	3840
	N	3560	4400		3896	4022
	N	3600	4200		3840	3930
	N	3500	4480		3892	4039
	N	3780	4280		3980	4055
Kyrgyz Front Range	E	3660		3840		
	N	3520		3760		
	N	3600		3740		
	N	3440		3900		
	NNE	3440		3860		
	NE	3380		3600		
	N	3300		3760		
	N	3400		3760		
	NNW	3260		4000		
	NNW	3400		3900		
	WNW	3400		4120		
	NW	3120		4000		
	E	3200		4450		
	SE	3060		3680		
	NNW	3360		3840		
	N	3200		4300		
	E	3440		4160		
	N	3550		3920		
	N	3560		3920		
	N	3400		4000		
	N	3420		4000		
	N	3560		4000		
	NNE	3780		4000		

Please cite this article as: Koppes, M., et al., Late Quaternary glaciation in the Kyrgyz Tien Shan. Quaternary Science Reviews (2008), doi:10.1016/j.quascirev.2008.01.009

Table 3 (*continued*)

Range	Aspect	Glacier toe altitude	Headwall altitude	Snowline altitude[d]	ELA ($THAR_{0.4}$)[a]	ELA ($THAR_{0.55}$)[c]
	NNW	3440	4000	3690	3664	3748
At Bashi Range	N	2415	4470		3237	3545
	N	3600	4320	3840		
	N	3440	4200	4100		
	N	3600		4200		
	N	3675		4000		
	N	3580		3800		
	N	3360		3600		
	S	4040		4240	4152	4194
	SE	3850		4045	3990	4043
Torugart Range	N			4159		
	N			4205		
	N			4229		
	N			4186		
	N			4271		
Mustyr			4653			

Modern toe and headwall elevations were initially calculated from 80-m contours on the 1:200,000 scale topographic maps and verified from late-summer snowlines visible on the Corona satellite images. Precision was on the order of ± 160 m. These data were later refined using ASTER DEMS with ~10-m accuracy. Toe elevations for former glaciers were taken from GPS measurements on the crest of LGM terminal moraines.

[a]ELA is calculated as 40% of the distance between the toe and headwall altitudes. Headwall altitudes are taken to be modern values.

[b]Altitude of the highest lateral moraine.

[c]ELA is calculated as 55% of the distance between the toe and headwall altitudes. Headwall altitudes are taken to be modern values.

[d]Firn line measured from Corona satellite images and 1:200,000 topographic maps.

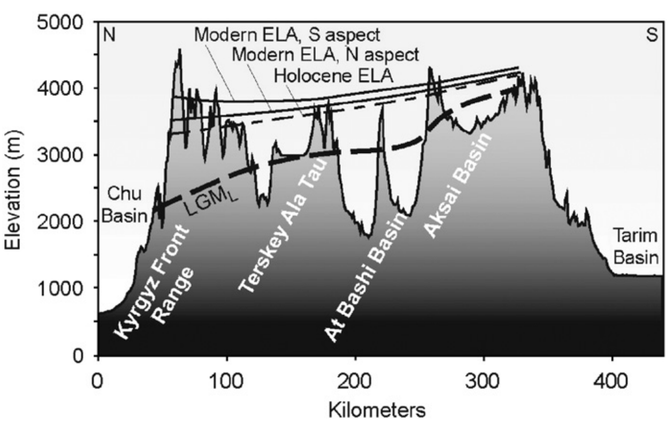

Fig. 7. North–south topographic profile across the Kyrgyz Tien Shan showing the discordant modern and paleo-equilibrium-line altitudes (Table 3). The profile was generated from NASA's SRTM DEM.

The lower moraine IV (CS-102, 3180 m), is double-crested and composed of fresh granite and meta-conglomerate clasts in a sandy silty matrix. The boulders were little-weathered and lichen-covered, and moraine slopes were less than the angle of repose (interior ~30° and exterior ~20°). The higher moraine V (CS-101), at 3246 m, was similarly composed. Both interior and exterior slopes were over-steepened (40° average). There was no loess cover.

The neighboring Chor Kyrchak Valley was also extensively glaciated. Less steep and lacking the large Ala Archa River, moraine preservation is better. An LGM_L moraine (III) there was mantled by over 45 cm of loess, a single depositional unit. Loess deposition appears to have been faster than in the Terskey Ala Tau to the east, possibly because of greater proximity to the Chu Basin and Kazakh steppe. Although it is not clear that the loess mantled an uneroded surface, a quartzite cobble (CS-104) was extracted from the buried surface at the base of the loess for cosmic-ray exposure dating. Young moraines (V?) and active glaciers are found upvalley.

Correcting for burial, and assuming a loess density of 1.8 g/cm^3, the cobble yielded an apparent age of ~50 ka. Single ^{10}Be analyses of granitic boulders on Ala Archa moraines IV and V yielded ages of 0.5 and 0.2 ka, respectively. Differential weathering and erosion on moraine IV appears greater than can explain such a small age difference. The dating of moraine V is consistent with its fresh geomorphic appearance, and it at least must date to the LIA.

The ELA for the LGM_L glacier in Chor Kyrchak Valley was ~2450 m. Relative to a modern ELA of 3870 m, the ELA depression for the LGM_L was ~1420 m. The ELA depression for Ala Archa advance IV was 280 m; for the LIA it was 170 m. Modern vegetation and the asymmetric incision of the Kyrgyz Front Range suggest a strong rain-shadow effect from north (wetter) to south (drier) across the range. The modern ELA on the south side of the range is ~3970 m, about 100 m higher than to the north, consistent with this suggestion. In contrast, the LGM_L ELA depression there is ~630 m, about half the northern value, possibly indicating a stronger rain shadow during the late Pleistocene.

Please cite this article as: Koppes, M., et al., Late Quaternary glaciation in the Kyrgyz Tien Shan. Quaternary Science Reviews (2008), doi:10.1016/j.quascirev.2008.01.009

5.4. At Bashi (Fig. 5)

The end moraines of the LGM_L glacier advance (III) in the Terekçu Valley are simple ridges, nearly closed, that end on the upper piedmont, at 2365 m. The left-lateral LGM_L moraine buried an older drift that was assigned to Unit II. The Unit II drift does not form distinct moraines, and may represent a degraded piedmont complex. Small inset recessional moraines of Unit III lie within 2 km of the end moraine. No stagnant-ice terrain was apparent. Both the II and III moraines are mantled by up to 60 cm of loess, measured in gullies on the outer flank of the left-lateral moraines. Loess deposition appeared to be slower than to the north and south. Soil development on both II and III moraines is minimal.

A few large schistose boulders with quartz veins are preserved on the moraine II and III crests; all were moderately weathered. The vein quartz from three boulders on the left-lateral LGM_L moraine and two boulders on the underlying piedmont-type moraine were sampled, yet only one sample from each moraine yielded enough quartz for cosmic-ray exposure dating. The boulders dated to 53 ka on moraine II and 32 ka on moraine III ("max" ages).

Two moraines are preserved in the main Terekçu Valley between the LGM_L and the modern glacier. The lower, ending at 3525 m, is sparsely vegetated. We assigned this moraine to Unit IV. The end moraine is eroded, but the left-lateral moraine is a prominent ridge rising above the modern glacier. A higher moraine (V) ends at 3670 m, at which point the Unit IV glacier was already >75 m thick. The modern, clean-ice glacier terminates at 3730 m. Moraine IV may be a partially deflated rock glacier, with a rubbly center lower than the lateral moraines, but retaining an ice core.

The firn line altitude of the modern glaciers of the At Bashi Range is ~4040 m; calculated ELAs are ~30 m lower. The ELA of glacier II was ~3300 m, giving an ELA depression of ~710 m. The ELA of the LGM_L glacier III was ~20 m higher. Moraine IV gives an ELA depression of ~110 m; moraine V gave a depression of ~45 m.

5.5. Aksai (Fig. 6a)

The LGM_L glaciers (III_a and III_b) of Djo Bog Gulsh Valley advanced onto the upper piedmont of Aksai Basin, nearly coalescing with those of adjacent valleys. At least two earlier generations of moraines protrude from beneath the LGM_L moraines. Apparently, the debris load of the Aksai glaciers fluctuated. Glaciers of Unit I formed a stagnant-ice piedmont lobe that left behind a complex deposit of drift with kettles. In contrast, glaciers of Units II and III_a appeared to be debris-poor, and left behind simple ridge moraines and little ground till. Unit III_b again was debris-rich. With a dominantly schistose lithology, there were few boulders available for ^{10}Be dating.

Loess cover on all units is extensive, and deposition was significant. Moraine I is capped by over 1.3 m of loess, in two packets. The lower packet (~1.0 m thick) contains non-pedogenic carbonate throughout; the upper packet (~0.35 m), overlying a sharp unconformity, contains no carbonate and shows less soil color. In contrast, the moraines II and III_a are capped by only the thin, carbonate-free upper loess.

The valleys above III_b end moraines are clean, with no recessional moraines and little ground till, until small rock glaciers are encountered above ~3900 m. A few modern glaciers remain, but most of the cirques are ice-free. The modern glaciers appear to be cold-based, with steep slopes and near-vertical termini. Multiple ridges of rocky till can be found below some of them, probably dating from the LIA (Unit V). These Unit V glaciers were probably avalanche-fed, and hence do not yield useful ELAs.

Above 3730 m altitude on the western tributary valley are three side-wall moraines or protalus ramparts (Unit V). The lowest is a thin veneer over bedrock, capped with up to 75 cm of poorly developed soil. The second is at 3804 m, and has a slope of 23°. It comprises subangular clasts of marble, schist and granite with only minor carbonate scale, and is capped with 7 cm of soil and up to 40 cm of clay-rich loess. The third moraine, at 3879 m, has a slope of 34°. No carbonate coating was found on clasts. The till was capped with 10–15 cm of loess over ~20 cm of clay-rich till, below which is a clast-supported till of the same composition as the lowest of the three moraines. Exposed clasts are lichen-covered.

A large granitic boulder on the crest of the left-lateral LGM_L moraine (CS-66) gave a cosmic-ray exposure age of 37–39 ka. A granitic boulder from the crest of moraine V (CS-61) yielded an exposure age of ~7.4 ka. Two granitic boulders from the higher moraine of CS-62 moraine yielded cosmic-ray exposure ages of 4.6 and 4.4 ka.

In a sheltered position at the head of the drainage the remnant of a cirque glacier terminates at 3950 m, with an ELA of ~4150 m. The ELA inferred from highest occurrence of the LGM_L lateral moraine is 3760 m, in close agreement with the THAR value of 3780 m. The ELA depression for III_b was 400 m; for moraine III_a it was 440 m. The earlier advances I and II had ELA depressions of the same magnitude as III_a and III_b.

5.6. Mustyr (Fig. 6b)

The Mustyr River exits the Torgurat Range to the north and incises to a depth of 20 m the extensive post-LGM_L outwash terraces on the piedmont. The terraces contain up to 5 m of lodgment till overlying stratified gravels. They lie between broad (~1.3 km), low (~90 m) LGM_L moraines (Unit III). On the basis of morphology, the right-lateral moraine appears to be composed of two separate ridges (III_a and an inset III_b). The right-lateral III_a moraine is bordered by drift left from the stagnant ice of a debris-rich piedmont glacier, also assigned to Unit III on the basis of weathering and morphology. The piedmont drift forms two broad moraines, distinguished only topographically, and we regard the moraines as belonging to Unit III_b. Behind the moraines is drift, probably supra-glacial till, in a complex terrain of kettles and ridges. The inset right-lateral III_b moraine also has stagnant-ice topography, in which it differs from the older III_a moraine and the younger terraces. This moraine may be from an outlet glacier from the piedmont lobe, and therefore we regard the two moraines as being from the same advance. The highest LGM_L lateral moraine was at ~3900 m. Soil development on all LGM_L moraines was minimal, and loess cover averaged <10 cm on ridge crests and up to 30 cm in flats near the lower ends of the moraines at 3550 m altitude.

A low, striated bedrock ridge emerges from beneath the most extensive Mustyr terrace at 3450 m. It is partly covered by a thin layer of drift. The terraces bifurcate near this ridge, and the gravelly plain between them does not appear to be of glacial origin. In addition, we found no evidence of older I and II drift which was so prominent at Aksai. We infer that moraines I and II were less extensive than, and buried by, moraines of Unit III. The striated ridge appears to be near the lower limit of the LGM_L glaciers.

In the upper Mustyr Valley, moraines of Units IV and V are found down to altitudes of 3650 and 3850 m, respectively. Unit IV is represented by complex low and vegetated moraine ridges, but moraines of Unit V are larger and bare. Modern glaciers overflow their cirques, terminating at altitudes of ~4140 m. The absence of quartzose rocks in the dominantly marble Torgurat Range made ^{10}Be dating at Mustyr unfeasible.

ELAs of the LGM_L (III) glaciers were about the same, ~3990 m, only 90 m higher than highest lateral moraine. ELAs for Units IV and V were 4075 and 4160 m, respectively. Modern ELAs average 4340 m. LGM_L ELA depressions were ~350 m, about 50 m less than at Aksai, only 100 km to the east. ELA depressions lessened to 265 m and 245 m for Units IV and V.

Despite the non-glaciated character of the southern side of the range, where small south-facing glaciers occur, their ELAs are only ~20 m higher than on the north side. However, glaciers on the north side of the Ferghana Range, 50 km to the northwest, have modern ELAs of ~4040 m, 300 m lower than in the Torgurat Range. Equivalent ΔELAs for Units III, IV and V in the Ferghana Range were ~330, ~190, and ~110 m, respectively.

6. Discussion

Given the limited time that was available for field interpretation, the necessary reliance on photo-interpretation for verification, and the need to spread limited funding for cosmic-ray exposure ages among the many field sites, we regard our results as reconnaissance in nature only. This is particularly true given the limited number of exposure ages we could obtain from each moraine sequence, which did not allow for sufficient checking for erosion and burial, and therefore should be considered untrustworthy as absolute landform ages. These caveats aside, we observed essentially similar sequences of moraines in all the studied drainages. All moraines preserved their original morphology, with little sign of landform erosion or relaxation. Most were capped by 0.5–2 m of loess. Although wide scatter in the ^{10}Be ages on some of the older moraines suggest potential landform disturbances, such as burial or erosion, the age of the moraines within each drainage followed the same pattern, getting progressively younger upvalley (Figs. 8 and 9).

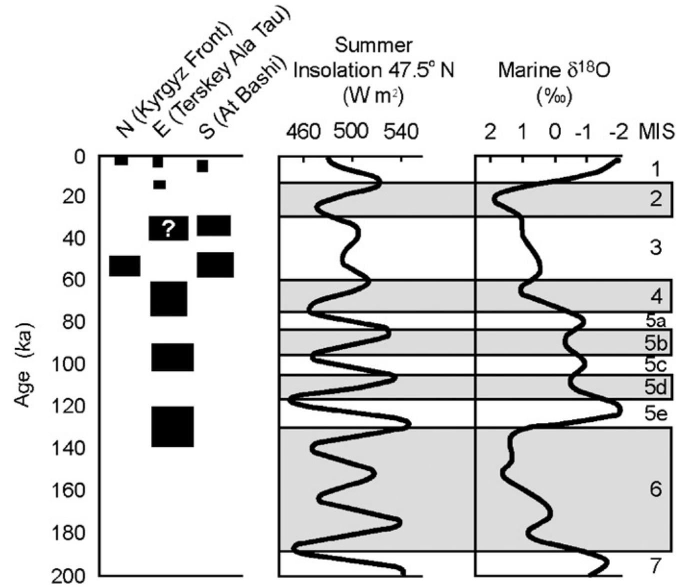

Fig. 8. Glacier advances in different parts of the Kyrgyz Tien Shan vs. summer insolation (Berger and Loutre, 1991) and the marine oxygen isotope record (Imbrie et al., 1984).

6.1. Apparent ages

The LGM_L throughout the Kyrgyz Tien Shan appears to have been ~37 ka or older, preceding the global LGM_G significantly, by tens of thousands of years. This is the same pattern reported by Owen et al. (2005) on the Tibetan Plateau and in earlier studies of the Hunza and Chitral regions in the monsoon-influenced southwestern slopes of the Karakoram in Pakistan (e.g., Benn and Owen, 1998; Finkel et al., 2003). This pattern of a pre-MIS 2 maximum advance also agrees with the ^{10}Be and ^{26}Al ages for moraines in the Karakax Valley of the Kunlun, south of the Tarim Basin (Clark et al., 2001). Boulders from the oldest moraines we were able to date came from the Terskey Ala Tau and produced ages of ~139–134 ka in Ala Bash and 155 ka in the Gulbel drainage. Boulders from the LGM_L were dated at 70–64 ka, similar to the dates from the LGM_L in the Garwhal Himalaya (Sharma and Owen, 1996). However, boulders from moraines of equivalent size in the southern At Bashi Range produced ages of only 37–32 ka, co-eval with inferred warmer and moister climatic conditions in the region during ~38–30 ka (MIS 3), recorded in the Dunde and Guliya ice caps (Thompson et al., 1989, 1990, 2006), and in OSL dates of lacustrine sediments interbedded with aeolian deposits in the central Taklamakan (Yang et al., 2006).

Glacier advances during MIS 2, if any, appear to have been restricted to the upper reaches of the valleys, a pattern not familiar in studies of mountain glaciations of Europe, the Americas, or even the Central Himalaya. We found evidence of only one MIS 2 cirque glacier advance, in Ala Bash. Many of the drainages in the southern and eastern ranges of the Kyrgyz Tien Shan appeared to be till-free between the LGM_L moraines and the modern cirques. The cirque moraines we dated at Aksai were formed in the late Holocene, and the glaciers that created them must have over-ridden any MIS 2 moraines. The asynchrony between the LGM_L and LGM_G implies that relative dating by correlation with distant glacial chronosequences is error-prone in Central Asia.

Advances in the upper cirques of the Aksai and Ala Bash Basins occurred in the mid to late Holocene. Our dates of MIS 1 advances do not appear to reflect an early Holocene advance around 9 ka, as was documented in the inner Tien Shan by Bondarev et al. (1997). We did, however, find a similar, steady decrease in cirque glacier size throughout the Holocene.

6.2. ELA patterns

A topographic profile across the Kyrgyz Tien Shan with the modern, Holocene and LGM_L ELAs for the studied drainages is shown in Fig. 7. The timing of the LGM_L in Kyrgyzstan appears to have varied significantly across the region, although our reconnaissance-level dating does not support a detailed analysis of the ELA trends during any single Pleistocene stage. The altitude of the LGM_L end moraines rose steeply from around 2000 m along the northern Kyrgyz Front Range, to 2600 m on the northern flank of the At Bashi Range, to 3400–3500 m in the south. The glaciers in the Terskey Ala Tau appear to have descended to around 2900–3000 m during the penultimate glacier advance, and to 2500–2600 m in the last glacial advance, similar to the northern flank of the more southerly At Bashi Range.

The ELAs for the modern glaciers show a pronounced gradient, both north–south and west–east, rising from ~3800 m in the north of the range, to 4000 m in the east and 4200 m in the south. The ELAs for the LGM_L glaciers also follow the same pattern, albeit with a more pronounced gradient: the ELA depression decreases from 1350 ± 150 m in the north, to 1000 ± 150 m in the east, to 400 ± 100 m in the south. This pattern suggests the presence

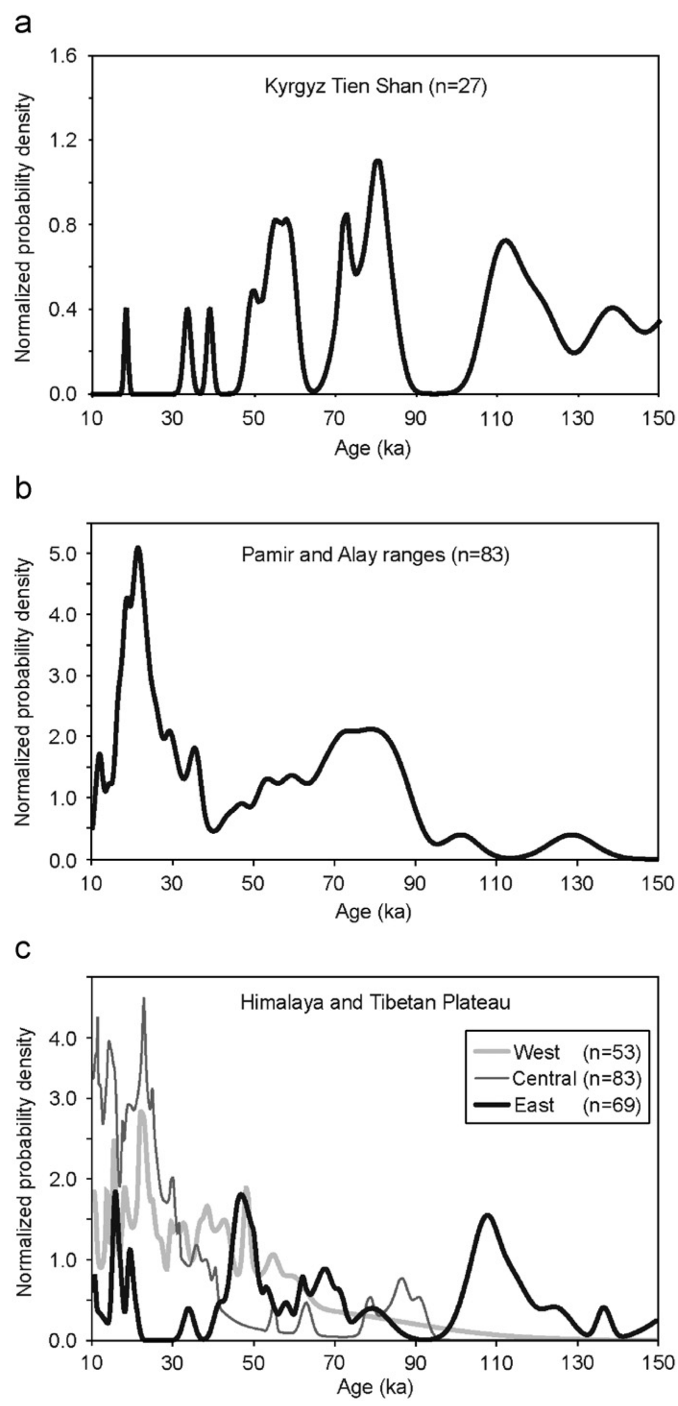

Fig. 9. Summed histograms of Pleistocene ^{10}Be cosmic-ray exposure dates from the Kyrgyz Tien Shan and neighboring areas. Probability distributions for individual dates have been normalized so that the probability mass function for each sample is one, with a maximum probability (at the mean value) of ~0.395; thus, the summed probability is related to the number of samples. Systematic uncertainties have not been included. (a) Kyrgyz Tien Shan (this study). (b) Pamir and Alay Range of western Kyrgyzstan. Ages plotted are "maximum" (erosion rate of 3 mm/ka) age ranges of Abramowski et al. (2006). The Kyrgyz Tien Shan and the Pamir/Alay differ at >99% confidence (Kolmogorov–Smirnov two-tailed test based on randomizing the actual dates 100 times). (c) Himalaya and the Tibetan Plateau. "West" includes Hunza, Chitral and Nanga Parbat (Phillips et al., 2000; Owen et al., 2002a, b); "Central" includes Mt. Everest, Khumbu, NW Garwhal and Lahul Himalaya (Sharma and Owen, 1996; Richards et al., 2000; Owen et al., 2001; Finkel et al., 2003); "East" includes the Tanggula Shan, Nyainqentanggulha Shan and Gonga Shan in eastern Tibet (Owen et al., 2005). It should be noted that several different scaling models and production rates were used in these studies; only reported ages are plotted here.

of a strong rain-shadow effect that prevailed during glacial times, with moisture delivered to the Tien Shan primarily from the northwest, and moisture from other directions blocked by the high Ferghana Range and the Pamir to the west and southwest and by the Tibetan Plateau and Karakorum to the south. The timing of the LGM_L also varies significantly, with the largest advance occurring at ~65–50 ka in the northern and eastern portions of the range, and at ~35 ka in the southern part of the range.

In the Kyrgyz Tien Shan, on several occasions the glaciers advanced to about the same positions, thousands of years apart, perhaps in different stages, and possibly even in different glacial cycles. This pattern has also been observed in Europe and North America (e.g., Gillespie and Molnar, 1995; Kaufman et al., 2004), in more maritime climatic regimes, but not to the extreme that we see in Kyrgyzstan. However, in Kyrgyzstan during MIS 2 the ELA raised and glaciers were restricted to the upper reaches of the valleys. The ELA remained high throughout the Holocene. In the Alps or the Sierra Nevada, the ELA did not rise until after MIS 2 (e.g., Kaufman et al., 2004). The Kyrgyz pattern matches findings in the high Himalaya and southern Tibetan Plateau (e.g., Sharma and Owen, 1996; Phillips et al., 2000; Richards et al., 2000; Owen et al., 2002a, b, 2003a, b, 2005), where it has been postulated that a drop in Monsoon intensity during MIS 2 counterbalanced any potential to increase glacier mass balance due to cooler temperatures.

6.3. Debris content and loess accumulation

The LGM_L moraines in the Kyrgyz Tien Shan often appear as a doublet, as has been documented in the Xinjiang Tien Shan (Gillespie and Burke, 2000), with the inner moraine a simple parabola enclosing the vanished glacier, and the outer, higher moraine more complex and enclosing dead-ice terrain with numerous kettle depressions, eskers, rogen moraines, outwash and fluvial terraces. In the Ala Bash and Djo Bog Gulsh (Aksai) drainages, a single, inset moraine was found between the large LGM_L terminus and the upper cirques, interpreted in the field to be an LGM_L recessional moraine. This "recessional" moraine had the debris-rich, stagnant-ice form attributed to the older glacier advances in Djo Bog Gulsh, Ala Bash and Mustyr. Evidence of deposition of debris-rich stagnant ice following the LGM_L was absent in the other basins.

The loess that mantles the Aksai moraines sheds some light on conditions during and after glacial advances. The moraines of the pre-LGM_L advance (Unit I) were debris-rich, as judged from the massive deposits of till, and were mantled by non-pedogenic carbonate-rich loess, which must have had a distant provenance, as the local source rocks in the Aksai Basin are limited to schists and granites and thereby low in carbonate. This distant source, probably dried lakes of the Kazakh steppes or the deserts around the Aral and Caspian seas, dominated any local sources of silt. High production of distant loess implies dry, windy conditions on the steppe, with low lake levels and sparse vegetation, at some point after the pre-LGM_L glaciation and possibly during the colder, drier Unit II re-advance (as indicated by the debris-poor Unit II moraine). Low local silt accumulation during this period also implies windy local conditions, capable of removing any local silt produced from the debris-rich pre-LGM_L advance.

The debris-rich LGM_L advance (Unit III) in Aksai Basin around 36 ka, unlike the (undated) pre-LGM_L advance, was capped by only a carbonate-free loess of local provenance. This carbonate-free loess also blanketed the pre-LGM_L advance landforms. This is consistent with warmer conditions during MIS 3, with warm-based glaciers generating more silt and debris, followed by a return to cold and dry conditions after 36 ka, promoting dust deposition. Such conditions appear to have been typical during MIS 2 over much of Central Asia. The absence, or significant decrease of non-pedogenic carbonate from distal sources during this period may suggest that either the steppes and desert to the northwest were frozen, effectively blocking loess generation or, perhaps, westerly storm tracks drifted further north due to a smaller Fenno-Scandian ice sheet. It is remarkable that, despite these inferred climatic differences during and between the last few maximum advances, the ELA depression during each glacial advance remained about the same.

6.4. Source of loess

It is widely assumed that the source for Central Asian loess is the Gobi Desert (e.g., Liu, 1985; Dodonov, 1991; Dodonov and Baiguzina, 1995) and the Taklamakan (e.g., An et al., 1991; Porter, 2001). The presence of thick caps of loess on the northern flank and in the upland basins of the Kyrgyz Tien Shan, upwind from the Gobi, implies that some of the silt in the loess plateau of China may have originated in the steppes north and west of the Kyrgyz Tien Shan, and fluctuations of that fraction through time may give new insights into wind strength and storm tracks during the major climatic reorganizations in the region.

6.5. Implications for paleo-climate

Today, the main sources of precipitation in Kyrgyzstan are cyclonic storms driven by westerly winds (Hodges et al., 2003). In both the Kyrgyz and Xinjiang Tien Shan, the mass balance of glaciers is positive in the spring and fall, and negative in summer and in winter (Liu and Han, 1992). This pattern is distinct from the one for less-continental regions, where a positive winter mass balance is a key factor in glacier maintenance. The negative mass balance in winter in the Xinjiang Tien Shan has been attributed to the presence of the Siberian thermal high-pressure system (Li et al., 2003), with its clear conditions and cold, dry air, diverting storms to the south and enhancing sublimation. This pattern was probably most pronounced during MIS 2, when the growth of the Fenno-Scandian ice sheet shifted

Please cite this article as: Koppes, M., et al., Late Quaternary glaciation in the Kyrgyz Tien Shan. Quaternary Science Reviews (2008), doi:10.1016/j.quascirev.2008.01.009

the major storm tracks to the south (e.g., Dodonov and Baiguzina, 1995; Hubberten et al., 2004; Svendsen et al., 2004), and when lower temperatures increased the duration of the thermal high-pressure systems over Siberia. Permafrost as far south as the Gobi reduced soil moisture recycling during the brief summers. The lack of evidence of significant glacier advances during MIS 2 in the Pamir and Karakoram (e.g., Owen et al., 2002a, b; Abramowski et al., 2006), presumably targets for precipitation from the southerly MIS 2 storms, suggests that moisture delivery was restricted across all of Central Asia during the LGM_G.

The modern ELA gradients in the Kyrgyz Tien Shan suggest a strong rain shadow, with moisture being delivered primarily from the northwest, and moisture from other directions being blocked by the high Ferghana Range and the Pamir to the west and southwest, and by the Tibetan Plateau and Karakorum to the south. The monsoon does not reach the Kyrgyz Tien Shan.

The more pronounced ELA gradients for the LGM_L glaciers may also result from moisture blocking. In terms of earlier climatic interpretations, the difference in the timing of the LGM_L across Kyrgyzstan suggests a southward shift in westerly storm tracks during the late Pleistocene, driving precipitation southwards. Rupper (2007) cautions that in continental environments temperature, not precipitation, often controls glaciation. Even if precipitation is generally a subordinate control, however, the strong ELA trends we describe suggest that in Kyrgyzstan it may have been important.

The rise of ELAs during MIS 2 in Kyrgyzstan must have reflected a strong forcing function. The restriction of MIS 2 glaciers to cirques is inconsistent with dominant temperature control, for by all accounts Central Asia was much colder as the last glacial cycle progressed. Rupper (2007) points out that in low-precipitation regimes, sublimation can be the dominant ablation process, such that summer cloudiness (for example) plays an unusually important role in ELA. Complications such as this make inference of climatic conditions from glacier ELAs less certain. However, even though the MIS 2 Kyrgyz Tien Shan appears to be a likely candidate for a sublimation-dominated regime, it is difficult to avoid the conclusion that the arid late Pleistocene environment in Central Asia was the main factor in the small glacier sizes. Thus, the paleo-ELA patterns we found, with large ELA depressions in the west and north of the range and smaller depressions in the east and south, may suggest that (1) precipitation in the late Pleistocene arrived in the Kyrgyz Tien Shan from the northwest and west, similar to the present, and (2) the growth of glaciers in the region were less controlled by temperature than by precipitation changes.

Modern glaciers in the Kyrgyz Tien Shan are mostly warm-based (Savoskul, 1997), in contrast to cold-based glaciers at similar altitudes and latitudes but farther east in Xinjiang (Kunakhovitch and Sokalskaya, 1997; Zhang et al., 1998). These modern glaciers are most likely about the same size as the MIS 2 glaciers that advanced during the coldest part of the late Pleistocene. The presence of larger warm- and cold-based Pleistocene glaciers emphasizes the complex relation between ELA and climatic conditions, and the difficulty of inverting ELA data to infer regional climatic conditions in Central Asia, given that the transition from cold- to warm-based glaciers and back to cold-based appears to be transgressive in both time and space.

7. Conclusions

The Kyrgyz Tien Shan was extensively and repeatedly glaciated during the late Pleistocene. The northern ridges of the Kyrgyz Tien Shan are the first high ground intercepted by winter storms crossing the plains of eastern Europe and Central Asia, and the ELA rises rapidly southeast of this barrier. The trend in the ELA was even more pronounced during the local Last Glacial Maxima. The range is the leading edge of the rain shadow that contributes to the arid and hyperarid core of Central Asia, in the Taklamakan and the northwestern Tibetan Plateau. Climatic inferences made from the distribution of glaciers and ELA trend surfaces must therefore take this rain-shadow effect into account.

Glaciers in the Kyrgyz Tien Shan appear to respond primarily to changes in precipitation rather than reduced regional temperatures, as indicated by the apparently small size of any MIS 2 glaciers across the range. Glacier advances in the Tien Shan were most probably driven by storms delivering moisture from the Kazakh steppes and the Mediterranean. Although the number of exposure ages we were able to collect across the range were limited, and this study should hence be considered reconnaissance in nature only, our preliminary results indicate the timing of the largest glaciations in the area correspond to inferred warmer climatic conditions in the region during MIS 3 through MIS 5, during periods of maximum summer insolation and minor global cooling.

The local LGM_L in the Kyrgyz Tien Shan appears to predate the global LGM_G by tens of thousands of years and parallels the local glacial maxima on the Tibetan Plateau and in the high mountain ranges to the south. The timing of the last large glaciations in the region, which dated at around 98 and 64 ka in the eastern part of the range, 49 ka in the northern part of the range, and 35 ka in the southern portion, suggests that local glaciations are out of phase not only with the mountain glaciations in Europe and North America, but also with the advances of the high-latitude ice sheets. Asynchronism in the Kyrgyz Tien Shan is manifest not only in the timing of the LGM_L but also in the overall pattern of ELA depression relative to modern values, compared to glaciers in Europe and North America. The temporal pattern of ELA depression generally suggests simple regional cooling driving transitions between cold- and warm-based glaciers, but such inferences will require further testing with global climate models.

Acknowledgments

We thank the late Yuri Trapezhnikov, Valentina Sankova, Keira Armstrong, Reed Burgette, Kanatbek Abdrakhmatov, and Gennadi Voromov for help and logistical support in the field and Laura Gilson for help with the figures. We also thank Gerard Roe and Summer Rupper for stimulating discussion of climatic interpretations in the region. This research represents one phase of a project on Central Asian paleo-climate sponsored by the NASA EOS/ASTER program (Contract NNG04HZ55C to Gillespie). Funding for Koppes was by grants from the Geological Society of America, the University of Washington Graduate School and the University of Washington Department of Geological Sciences. Support for Thompson was provided by grant EAR 9614412 from the NSF Continental Dynamics program.

References

Abramowski, U., Bergau, A., Seebacha, D., Zech, R., Glaser, B., Sosin, P., Kubik, P.W., Zech, W., 2006. Pleistocene glaciations of Central Asia: results from ^{10}Be surface exposure ages of erratic boulders from the Pamir (Tajikistan), and the Alay–Turkestan range (Kyrgyzstan). Quaternary Science Reviews 25, 1080–1096.

Adyshev, M.M., Kashirin, F.T., Umurzakov, S.U., Almaev, T.M., Voronina, A.F., Grigorenko, P.G., Dzhamgerchinov, B.D., Zabirov, R.D., Zin'kova, Z.Y., Izmajlov, A.E., Isabaeva, V.A., Kravchenko, A.B., Mamytov, A.M., Makhrina, L.I., Moldokulov, A.M., Murzaev, E.M., Otorbaev, K.O., Popova, L.I., Yar-Mukhamedov, G.H., Yashina, V.V., 1987. Atlas of Kyrgyz S.S.R.: Natural Conditions and Resources, vol. 1. Central Administrative Board of Geodetics and Cartography, Council of Ministers, Moscow, 157pp.

Aizen, E.M., Aizen, V.B., Melack, J.M., Nakamura, T., Ohta, T., 2001. Precipitation and atmospheric circulation patterns at mid-latitudes of Asia. International Journal of Climatology 21, 535–556.

An, Z., Kukla, G.J., Porter, S.C., Xiao, J., 1991. Magnetic susceptibility evidence of monsoon variation on the Loess Plateau of Central China during the last 130,000 years. Quaternary Research 36, 29–36.

Balco, G., Stone, J.O.H., 2006. Muons for the masses: a simple, internally consistent, and easily accessible means of calculating surface exposure ages or erosion rates from ^{10}Be and ^{26}Al measurements. CRONUS-EARTH online url: 〈http://hess.ess.washington.edu/math/docs/al_be_stable/al_be_calc_paper_v2.pdf〉.

Balco, G., Dunai, T.J., Lifton, N.A., Stone, J.H., 2007. A complete and easily accessible means of calculating surface exposure ages or erosion rates from Be-10 and Al-26 measurements. Quaternary Geochronology, accepted, doi:10.1016/j.quageo.2007.12.001.

Benn, D.I., Lehmkuhl, F., 2000. Mass balance and equilibrium-line altitudes in glaciers in high mountain environments. Quaternary International 65/66, 15–29.

Benn, D.I., Owen, L.A., 1998. The role of the Indian summer monsoon and the mid-latitude westerlies in Himalayan glaciation; review and speculative discussion. Journal of the Geological Society of London 155, 353–363.

Benn, D.I., Owen, L.A., Osmaston, H.A., Seltzer, G.O., Porter, S.C., Mark, B., 2005. Reconstruction of equilibrium-line altitudes for tropical and sub-tropical glaciers. Quaternary International 138/139, 8–21.

Berger, A., Loutre, M.F., 1991. Insolation values for the climate of the last 10 million years. Quaternary Science Reviews 10 (4), 297–317.

Bondarev, L.G., Gobedzhishvili, R.G., Solomina, O.S., 1997. Fluctuations of local glaciers in the southern ranges of the former USSR: 18,000–8000 BP. Quaternary International 38/39, 103–108.

Burbank, D.W., Kang, J., 1991. Relative dating of Quaternary moraines, Rongbuk Valley, Mount Everest, Tibet; implications for an ice sheet on the Tibetan Plateau. Quaternary Research 36, 1–18.

Clark, D.H., Gillespie, A.R., Bierman, P.R., Caffee, M.W., 2001. Glacial asynchrony in the Kunlun Shan, northwestern Tibet. Geological Society of America, Abstracts with Programs 33 (6), 441.

Derbyshire, E., Li, J., Perott, F.A., Xu, S., Waters, R.S., 1984. Quaternary glacial history of the Hunza Valley, Karakoram Mountains, Pakistan. In: Miller, K. (Ed.), International Karakoram Project. Cambridge University Press, Cambridge, pp. 456–495.

Dodonov, A.E., 1991. Distribution and chronological problems of loess. GeoJournal 24 (2), 185–194.

Dodonov, A.E., Baiguzina, L.L., 1995. Loess stratigraphy of Central Asia: paleoclimatic and paleoenvironmental aspects. Quaternary Science Reviews 14, 707–720.

Ehlers, J., Gibbard, P. (Eds.), 2004. Quaternary glaciations—extent and chronologies. Part III: South America, Asia, Africa, Australia, Antarctica. Developments in Quaternary Science 2, 380.

Farr, T.M., Kobrick, M., 2003. The shuttle radar topography mission: introduction to the special session (abstract). In: American Geophysical Union/European Geophysical Society Annual Meeting, Nice, France.

Finkel, R.C., Owen, L.A., Barnard, P.L., Caffee, M.W., 2003. Beryllium-10 dating of Mount Everest moraines indicates a strong monsoonal influence and glacial synchroneity throughout the Himalaya. Geology 31, 561–564.

Gillespie, A.R., 1991. Testing a new climatic interpretation for the Tahoe glaciation. In: Hall Jr., C.A., Doyle-Jones, V., Widawski, B. (Eds.), Natural History of Eastern California and High-Altitude Research, Proceedings of the White Mountain Research Station Symposium, vol. 3, pp. 383–398.

Gillespie, A.R., Burke, R.M., 2000. Pre-LGM alpine glaciation in Central Asia. Geological Society of America, Abstracts with Program 32, 511.

Gillespie, A., Molnar, P., 1995. Asynchronous maximum advance of mountain and continental glaciers. Review of Geophysics 33, 311–364.

Gillespie, A.R., Burke, R.M., Clark, D.H., Mu, G., Wang, S., Yan, S., 1993a. Soil development on late Pleistocene glacial deposits in the Tien Shan, Western China. Geological Society of America, Abstracts with Program 25, 394.

Gillespie, A.R., Clark, D.H., Burke, R.M., 1993b. New interpretation of glacial sequences, Tian Shan, western China: implications for late Pleistocene snowline depression. Geological Society of America, Cordilleran-Rocky Mountain Sections, Abstracts with Program 25, 42.

Hodges, K., Hoskins, B., Boyle, J., 2003. A comparison of recent reanalysis datasets using objective feature tracking: storm tracks and tropical easterly waves. Monthly Weather Review 131 (9), 2012–2037.

Hoskins, B., Hodges, K., 2002. New perspectives on the northern hemisphere winter storm tracks. Journal Atmospheric Sciences 59, 1041–1061.

Hubberten, H.W., Andreev, A., Astakhov, V.I., Demidov, I., Dowdeswell, J.A., Henrikson, M., Hjort, C., Houmark-Nielsen, M., Jakobsson, M., Kuzmina, S., Larsen, E., Lunkka, J.P., Lysa, A., Mangerud, J., Moeller, P., Saarnisto, M., Schirrmeister, L., Sher, A.V., Siegert, C., Siegert, M.J., Svendsen, J.I., 2004. The periglacial climate and environment in northern Eurasia during the Last Glaciation. Quaternary Science Reviews 23, 1333–1357.

Imbrie, J., Hays, J.D., Martinson, D.G., Mclntyre, A., Mix, A.C., Morley, J.J., Pisias, N.G., Prell, W.L., Shackleton, N.J., 1984. The orbital theory of Pleistocene climate: Support from a revised chronology of the marine delta ^{18}O record. In: Berger, A., Imbrie, J., Hays, J., Kukla, G., Saltzman, B. (Eds.), Milankovitch and Climate, Part I. Reidel, Boston, pp. 269–305.

Kaufman, D.S., Porter, S.C. Gillespie, A.R., 2004. Quaternary alpine glaciations in Alaska, the Pacific Northwest, Sierra Nevada and Hawaii. In: Gillespie, A.R., Porter, S.C., Atwater, B.F. (Eds.), The Quaternary Period in the United States. Developments in Quaternary Science Vol 1 (series editor, J. Rose), Elsevier, pp. 77–103.

Kunakhovitch, M.G., Sokalskaya, A.M., 1997. The reaction of mountain glaciers to climatic change under continental conditions. Annals of Glaciology 24, 415–420.

Lal, D., 1991. Cosmic ray labeling of erosion surfaces: in-situ nuclide production rates and erosion models. Earth and Planetary Science Letters 104, 424–439.

Lehmkuhl, F., 1997. Late Pleistocene, Lateglacial and Holocene glacier advances on the Tibetan Plateau. Quaternary International 38/39, 77–83.

Lehmkuhl, F., 1998. Quaternary glaciations in central and western Mongolia. In: Owen, L.A. (Ed.), Mountain Glaciation, Quaternary Proceedings, vol. 6, pp. 153–167.

Lehmkuhl, F., Haselein, F., 2000. Quaternary paleoenvironmental change on the Tibetan Plateau and adjacent areas (western China and western Mongolia). In: Owen, L.A., Lehmkuhl, F. (Eds.), Late Quaternary Glaciation and Palaeoclimate of the Tibetan Plateau and Bordering Mountains. Quaternary International 65/66, 121–145.

Lehmkuhl, F., Owen, L.A., 2005. Late Quaternary Glaciation of Tibet and the bordering mountains: a review. Boreas 34, 87–100.

Li, Z., Han, T., Zhefan, J., Yang, H., Jiao, K., 2003. A summary of 40 years of observation data on Glacier No. 1 and climate change at the headwaters of the Urumqi River, Xinjiang, China. Journal of Glaciology and Geocryology 25 (2), 117–123.

Liu, D.S., 1985. Loess and Environment in China. Science Press, Beijing, 206pp.

Liu, C., Han, T., 1992. Relation between recent glacier variations and climate in the Tien Shan mountains, Central Asia. Annals of Glaciology 16, 11–16.

Meierding, T., 1982. Late-Pleistocene glacial equilibrium-line altitudes in the Colorado Front Range: a comparison of methods. Quaternary Research 18, 289–310.

Nishizumi, K., Winterer, E., Kohl, C., Klein, J., Middleton, R., Lal, D., Arnold, J., 1989. Cosmic ray production rates of 10-Be and 26-Al in quartz from glacially polished rocks. Journal of Geophysical Research 9, 17907–17915.

Owen, L.A., Benn, D.I., 2005. Equilibrium-line altitudes of the Last Glacier Maximum for the Himalaya and Tibet: an assessment and evaluation of results. Quaternary International 138/139, 55–78.

Owen, L.A., Gualtieri, L., Finkel, R.C., Caffee, M.W., Benn, D.I., Sharma, M.C., 2001. Cosmogenic radionuclide dating of glacial landforms in the Lahul Himalaya, Northern India: defining the timing of Late Quaternary glaciation. Journal of Quaternary Science 16, 555–563.

Owen, L.A., Finkel, R.C., Caffee, M.W., Gualtieri, L., 2002a. Timing of multiple glaciations during the Late Quaternary in the Hunza Valley, Karakoram Mountains, Northern Pakistan: defined by cosmogenic radionuclide dating of moraines. Geological Society of America Bulletin 114, 593–604.

Owen, L.A., Kamp, U., Spencer, J.Q., Haserodt, K., 2002b. Timing and style of Late Quaternary glaciation in the eastern Hindu Kush, Chitral, northern Pakistan: a review and revision of the glacial chronology based on new optically stimulated luminescence dating. Quaternary International 97/98, 41–56.

Owen, L.A., Spencer, J.Q., Ma, H., Barnard, P.L., Derbyshire, E., Finkel, R.C., Caffee, M.W., Zeng, Y.N., 2003a. Timing of Late Quaternary glaciation along the southwestern slopes of the Qilian Shan, Tibet. Boreas 32, 281–291.

Owen, L.A., Finkel, R.C., Ma, H., Spencer, J.Q., Derbyshire, E., Banard, P., Caffee, M.W., 2003b. Timing and style of late Quaternary glaciation in northeastern Tibet. Geological Society of America Bulletin 115, 1356–1364.

Owen, L.A., Finkel, R.C., Barnard, P.L., Ma, H., Asahi, K., Caffee, M.W., Derbyshire, E., 2005. Climatic and topographic controls on the style and timing of Late Quaternary glaciation throughout Tibet and the Himalaya defined by ^{10}Be cosmogenic radionuclide surface exposure dating. Quaternary Science Reviews 24, 1391–1411.

Phillips, W.M., Sloan, V.F., Shroder, J.F., Sharma, P., Clarke, M.L., Rendell, H.M., 2000. Asynchronous glaciation at Nanga Parbat, northwestern Himalaya Mountains, Pakistan. Geology 28, 431–434.

Porter, S.C., 2001. Chinese loess record of monsoon climate during the last glacial–interglacial cycle. Earth-Science Reviews 54, 115–128.

Richards, B.W.M., Benn, D.I., Owen, L.A., Rhodes, E.J., Spencer, J., 2000. Timing of late Quaternary glaciations south of Mount Everest in the Khumbu Himal, Nepal. Geological Society of America Bulletin 112, 1621–1632.

Rupper, S.B., 2007. Glacier sensitivity and regional climate: past and present. Ph.D. Dissertation, University of Washington, Seattle, USA, 205pp.

Rupper, S.B., Roe, G., 2007. Glacier sensitivity and regional climate: an energy balance approach. Journal of Climate, accepted.

Savoskul, O.S., 1997. Modern and Little Ice Age glaciers in 'humid' and 'arid' areas of the Tien Shan, Central Asia: two different patterns of fluctuation. Annals of Glaciology 24, 142–147.

Schäfer, J.M., Tschudi, S., Zhizhong, Z., Xihao, W., Ivy-Ochs, S., Wieler, R., Baur, H., Kubik, P.W., Schlüchter, C., 2002. The limited influence of glaciations in Tibet on global climate over the past 170 000 yr. Earth and Planetary Science Letters 194, 287–297.

Sharma, M.C., Owen, L.A., 1996. Quaternary glacial history of NW Garhwal, Central Himalayas. Quaternary Science Reviews 15 (4), 335–365.

Shi, Y., 2002. Characteristics of late Quaternary monsoonal glaciation on the Tibetan Plateau and in East Asia. Quaternary International 97/98, 79–91.

Solomina, O., Barry, R., Bodnya, M., 2004. The retreat of Tien Shan glaciers (Kyrgyzstan) since the Little Ice Age estimated from aerial photographs, lichenometric and historical data. Geografiska Annaler 86A (2), 205–215.

Stone, J.O., 2000. Air pressure and cosmogenic isotope production. Journal of Geophysical Research 105 (23), 723–753, 759.

Stone, J., 2004. Extraction of Al and Be from quartz for isotopic analysis. UW Cosmogenic Nuclide Lab Methods and Procedures. Online url: ⟨http://depts.washington.edu/cosmolab/chem.html⟩.

Svendsen, J.I., Alexanderson, H., Astakhov, V.I., Demidov, I., Dowdeswell, J.A., Funder, S., Gataullin, V., Henriksen, M., Hjort, C., Houmark-Nielsen, M., Hubberten, H.W., Ingo'lfsson, O., Jakobsson, M., Kjaer, K.H., Larsen, E., Lokrantz, H., Lunkka, J.P., Lysa, A., Mangerud, J., Matiouchkov, A., Murray, A., Moeller, P., Niessen, F., Nikolskaya, O., Polyak, L., Saarnisto, M., Siegert, C., Siegert, M.J., Spielhagen, R.F., Stein, R., 2004. Late Quaternary ice sheet history of northern Eurasia. Quaternary Science Reviews 23, 1229–1271.

Thompson, L.G., Mosley-Thompson, E., Davis, M.E., Bolzan, J.F., Dal, J., Klein, L., Gundestrup, N., Tao, T., Wu, X., Xie, Z., 1989. Holocene–late Pleistocene climatic ice core records from Qinghai–Tibetan Plateau. Science 246, 474–477.

Thompson, L.G., Mosley-Thompson, E., Davis, M.E., Bolzan, J.F., Dal, J., Klein, L., Gundestrup, N., Tao, T., Wu, X., Xie, Z., 1990. Glacial stage ice-core records from the subtropical Dunde ice cap, China. Annals of Glaciology 14, 288–297.

Thompson, S.C., Weldon, R.J., Rubin, C.M., Abdrakhmatov, K., Molnar, P., Berger, G.W., 2002. Late Quaternary slip rates across the central Tien Shan, Kyrgyzstan, Central Asia. Journal of Geophysical Research 107 (B9), 2203.

Thompson, L.G., Mosley-Thompson, E., Davis, M.E., Mashiotta, T.A., Henderson, K.A., Lin, P.N., Yao, T., 2006. Ice core evidence for asynchronous glaciation on the Tibetan Plateau. Quaternary International 154/155, 2–10.

Yang, X., Preusser, F., Radtke, U., 2006. Late Quaternary environmental changes in the Taklamakan Desert, western China, inferred from OSL-dated lacustrine and aeolian deposits. Quaternary Science Reviews 25, 923–932.

Yi, C.L., Liu, K.X., Cui, Z.J., 1998. AMS dating on glacial tills at the source area of Ürümqi River in the Tianshan Mountains and its implications. Chinese Science Bulletin 43, 1749–1751.

Please cite this article as: Koppes, M., et al., Late Quaternary glaciation in the Kyrgyz Tien Shan. Quaternary Science Reviews (2008), doi:10.1016/j.quascirev.2008.01.009

Yi, C.L., Jiao, K.Q., Liu, K.X., Li, L., Ye, Y.G., 2002. ESR dating of the sediments of the last glaciation at the source of the Urumqi River, Tian Shan mountains, China. Quaternary International 97/98, 141–146.

Zhang, Y., Tao, T., Pu, J., 1998. The response of continental-type glaciers to climate change in China. Journal of Glaciology and Geocryology 20 (1), 3–8.

Zhang, W., Cui, Z., Li, Y., 2006. Review of the timing and extent of glaciers during the last glacial cycle in the bordering mountains of Tibet and in East Asia. Quaternary International 154/155, 32–43.

Zhao, J.D., Zhou, S.Z., Cui, J.X., Jiao, K.Q., Ye, Y.G., Xu, L.B., 2002. ESR dating of glacial tills at the headwaters of the Ürümqi River in the Tianshan Mountains. Journal of Glaciology and Geocryology 24, 737–743 (in Chinese with English abstract).

Zhou, S.Z., Li, J.J., Zhang, S.Q., 2002. Quaternary glaciation of the Bailang River valley, Qilian Shan. Quaternary International 97/98, 103–110.